Closed-Loop Transfer Recovery with Observer-Based Controllers

Part 2: Design

Ben M. Chen

Ali Saberi

School of Electrical Engineering and Computer Science
Washington State University
Pullman, Washington 99164-2752

Uy-Loi Ly

Department of Aeronautics and Astronautics, FS-10
University of Washington
Seattle, Washington 98195

I. INTRODUCTION & PROBLEM STATEMENT

The problem of closed-loop transfer recovery (CLTR) has been discussed in an early sequel paper [1]. The basic problem addressed there is the analysis of closed-loop transfer recovery using full-order and reduced-order observer-based controllers. The design objective is to recover using output feedback (if possible) the closed-loop transfer function achieved under a full-state feedback design for a given set of

CONTROL AND DYNAMIC SYSTEMS, VOL. 51

disturbance input and controlled output variables. To be specific, let us consider a plant Σ defined by

$$\Sigma : \begin{cases} \dot{x} = A\,x + B_1\,w + B_2\,u, \\ z = C_1 x + D_{11} w + D_{12} u, \\ y = C_2 x + D_{21} w + D_{22} u, \end{cases} \tag{1}$$

where $x \in \Re^n$ is the state, $u \in \Re^m$ is the control input, $w \in \Re^k$ is the disturbance, $z \in \Re^\ell$ is the controlled output and $y \in \Re^p$ is the measurement output. For convenience, we also define the subsystem Σ_{yw} to represent the matrix quadruple (A, B_1, C_2, D_{21}) and the subsystem Σ_{zu} for the matrix quadruple (A, B_2, C_1, D_{12}). We assume that the pair $(A,\ B_2)$ is stabilizable and the pair $(A,\ C_2)$ detectable. Without loss of generality, the following matrices $[C_1,\ D_{11},\ D_{12}]$, $[C_2,\ D_{21},\ D_{22}]$, $[B_1',\ D_{11}',\ D_{21}']'$ and $[B_2',\ D_{12}',\ D_{22}']'$ are assumed of maximal ranks. As shown in [1], one can also assume without loss of generality that $D_{22} = 0$ as well. Let F be a full-state feedback gain matrix such that under the state-feedback control

$$u = -Fx \tag{2}$$

(a) the closed-loop system is asymptotically stable, i.e. the eigenvalues of $A - B_2F$ lie in the left-half s-plane,

(b) the closed-loop transfer function from the disturbance w to the controlled output z, denoted by $T_{zw}(s)$, meets the desired frequency dependent design specifications.

We also refer to $T_{zw}(s)$ as the target closed-loop transfer function given by

$$T_{zw}(s) = (C_1 - D_{12}F)(\Phi^{-1} + B_2F)^{-1}B_1 + D_{11} \tag{3}$$

where $\Phi = (sI - A)^{-1}$. The problem of closed-loop transfer recovery (CLTR) is then to find an internally stabilizing output-feedback controller $\mathbf{C}(s)$ such that the recovery error defined as

$$E(s) := T_{zw}^o(s) - T_{zw}(s), \tag{4}$$

is either exactly or approximately equal to zero in the frequency region of interest. Here, $T_{zw}^o(s)$ represents the transfer function from w

to z of the closed-loop system. As discussed in Part 1 [1], achieving exact closed-loop transfer recovery (ECLTR) is in general not possible. Hence, it is more appropriate to examine situation where approximate recovery can be achieved. An approximate CLTR is tied to the notion that recovery can be achieved to any degree of accuracy. In this process, one normally parameterizes the controller $\mathbf{C}(s)$ as a function of a positive scalar parameter σ thereby generating a family of controllers $\mathbf{C}(s, \sigma)$. We say asymptotic CLTR (ACLTR) is achieved if

$$T_{zw}^{o}(s, \sigma) \rightarrow T_{zw}(s)$$

as $\sigma \rightarrow \infty$ pointwise in s, or equivalently

$$E(s, \sigma) \rightarrow 0$$

as $\sigma \rightarrow \infty$ pointwise in s. From the point of view of design, once the conditions of ACLTR have been verified, one should be able to find a controller $\mathbf{C}(s, \sigma)$ with a particular value of σ that produces the desired level of recovery.

In Part 1 [1], we consider the CLTR problem using a full-order observer-based controller of the form,

$$\begin{cases} \dot{\hat{x}} = (A - KC_2)\hat{x} + B_2 u + Ky, \\ u = -F\hat{x}, \end{cases} \tag{5}$$

and a reduced-order observer-based controller of the form,

$$\begin{cases} \dot{v} = A_{or} v + (B_{2,2} - K_{r1} B_{2,1})u \\ \qquad\qquad + [K_{r0},\ A_{21} - K_{r1} A_{11} + A_{or} K_{r1}] \begin{bmatrix} y_0 \\ y_1 \end{bmatrix}, \\ \hat{x} = \begin{bmatrix} 0 \\ I_{n-p+m_0} \end{bmatrix} v + \begin{bmatrix} 0 & I_{p-m_0} \\ 0 & K_{r1} \end{bmatrix} y, \\ u = -F\hat{x}, \end{cases} \tag{6}$$

where K and $K_r = [K_{r0}, K_{r1}]$ are respectively the full-order and reduced-order observer gain matrices. The submatrices in (6) are defined in equations (33) to (38) of Part 1. While it is recognized that in most cases neither ECLTR nor ACLTR can be achieved using either a

full-order or a reduced-order observer-based controller, the analysis of CLTR conducted in Part 1 provides however a detailed study of three fundamental issues related to the problem of CLTR. The first issue is concerned with what can and cannot be achieved for a given system and for an arbitrary target closed-loop transfer function. The second issue is to develop necessary and/or sufficient conditions for a target closed-loop transfer function to be recoverable either exactly or approximately. The third issue deals with the necessary and/or sufficient conditions on a given system such that it has at least one recoverable target closed-loop transfer function. Results of the analysis have identified some fundamental limitations of the given system as a consequence of its structural properties; namely, its finite and infinite-zero structure and invertibility. This enables designers to appreciate at the outset different design limitations incurred in the synthesis of output-feedback controllers; for example, how to select a meaningful set of measurements for the closed-loop transfer recovery design. Once we have chosen an appropriate set of measurement outputs, we can then proceed to the actual design of full-order or reduced-order observer-based controllers that will achieve as close as possible the desired target closed-loop transfer function. In this paper, we focus on three different design methods for closed-loop transfer recovery.

The paper is organized as follows. Section II reviews the necessary design constraints and the available design freedom. Section III develops the general ATEA method. Also, in section III, a simplified ATEA procedure is given for the design of exact closed-loop transfer recovery whenever it is feasible. Section IV examines design methods based on optimization. Here, two design methods have been considered; one that minimizes the H_2-norm of a recovery matrix while the other minimizes the respective H_∞-norm. Section V discusses the relative merits of ATEA and optimization-based designs. A numerical example based on a benchmark problem [16] is given in section VI, illustrating the practical usage of the analysis results in [1], and comparing different observer designs synthesized using methods discussed in sections III and IV. Conclusions are drawn in section VII.

As in [1], we adopt the following notations. A' denotes the transpose of A, A^H denotes the complex conjugate transpose of A, I denotes an identity matrix while I_k denotes the identity matrix of dimension $k \times k$. $\lambda(A)$ denotes the set of eigenvalues of A. Similarly, $\sigma_{max}[A]$ and $\sigma_{min}[A]$ denote respectively the maximum and minimum singular values of A. Ker$[V]$ and Im$[V]$ denote respectively the kernel and the image of V. The open-left, closed right-half s-planes and the $j\omega$ axis are denoted by $\mathcal{C}^-$, $\mathcal{C}^+$ and $\mathcal{C}^o$ respectively. Also, $\mathbf{T}^f_{\text{ER}}(\Sigma)$ denotes the set of exactly recoverable target closed-loop transfer functions for any given system Σ using a full-order observer-based controller, $\mathbf{T}^f_{\text{R}}(\Sigma)$ denotes the set of either exactly or asymptotically recoverable target closed-loop transfer functions, while $\mathbf{T}^f_{\text{AR}}(\Sigma)$ denotes the set of target closed-loop transfer functions which are asymptotically recoverable but not exactly recoverable for the given system Σ using full-order observer-based controllers. Precise definitions of $\mathbf{T}^f_{\text{ER}}(\Sigma)$, $\mathbf{T}^f_{\text{R}}(\Sigma)$ and $\mathbf{T}^f_{\text{AR}}(\Sigma)$ are given in [1].

II. DESIGN CONSTRAINTS AND FREEDOM

As shown in Part 1 [1], problem formulation of CLTR for the case of reduced-order observer-based controllers can be placed into the same framework as the one for full-order observer-based controllers. Thus, for simplicity of presentation, we will focus our development of CLTR design techniques only to the case of full-order observer-based controllers. In Part 1 [1], we have analyzed systematically when and under what conditions closed-loop transfer recovery (CLTR) is possible. According to the way we partitioned the recovery matrix [1], it is clear that any systematic design scheme for CLTR would involve, beside the requirement of closed-loop stability, placing some additional design constraints upon the observer gain matrix K. The goal is to make the recovery matrix as small as possible through a particular set of design constraints. Some constraints are related to the assignment of the finite, as well as the asymptotically infinite, eigenstructures of the observer dynamic matrix $A_o = A - K(\sigma)C_2$. After satisfying all the above constraints, some design freedom may still be left in the observer gain matrix K to

assign other parts of the eigenstructure in the matrix A_o.

To see this, we recall that the recovery error between the target closed-loop transfer function $T_{zw}(s)$ and the one realized by a full-order observer-based controller of (5) is given by

$$E_f(s,\sigma) = T_{zu}(s)M_f(s,\sigma) \tag{7}$$

where $T_{zu}(s)$ is the closed-loop transfer function from u to z under state feedback as defined in (19) of [1] and

$$M_f(s,\sigma) = F(\Phi^{-1} + K(\sigma)C_2)^{-1}(B_1 - K(\sigma)D_{21}). \tag{8}$$

The matrix $M_f(s,\sigma)$ is called the *recovery matrix*. It plays a dominant role in the analysis of recovery. In fact, if the system Σ_{zu} is left-invertible, then according to lemma 2 of [1] the recovery error $E_f(j\omega,\sigma)$ is zero if and only if the recovery matrix $M_f(j\omega,\sigma)$ is zero. Thus, the study of $M_f(s,\sigma)$ is tantamount to the study of CLTR. Assuming for simplicity that A_o is nondefective, one can express $M_f(s,\sigma)$ in the following matrix partial fraction expansion,

$$M_f(s,\sigma) = \sum_{i=1}^{n} \frac{R_i(\sigma)}{s - \lambda_i(\sigma)} \tag{9}$$

where $R_i(\sigma)$ is the residue matrix given by

$$R_i(\sigma) = FW_i(\sigma)V_i^H(\sigma)[B_1 - K(\sigma)D_{21}] \tag{10}$$

with $W_i(\sigma)$ and $V_i(\sigma)$ being respectively the right- and left-eigenvectors associated with the eigenvalue $\lambda_i(\sigma)$ of A_o. These eigenvectors are scaled such that

$$W(\sigma)V^H(\sigma) = V^H(\sigma)W(\sigma) = I_n$$

where

$$W(\sigma) = [W_1(\sigma),\ W_2(\sigma),\ \cdots,\ W_n(\sigma)]$$

and

$$V(\sigma) = [V_1(\sigma),\ V_2(\sigma),\ \cdots,\ V_n(\sigma)]. \tag{11}$$

As evident from (9) and (10), one can render the i-th term of $M_f(s,\sigma)$ zero in one of two ways:

(1) Render the residue $R_i(\sigma)$ zero while λ_i is finite; or

(2) Place λ_i asymptotically to infinity while keeping the residue $R_i(\sigma)$ uniformly bounded.

The first approach is the problem of finite eigenstructure assignment while the latter concerns eigenstructure assignment for the asymptotically infinite eigenvalues of A_o. From the structural properties of the system Σ_{zw}, there may not exist enough design freedom to assign the needed eigenstructure in A_o to achieve ECLTR or ACLTR. Analysis of Part 1 reveals several guidelines as to when, how and to what extent such an assignment can be done. To review these guidelines, $M_f(s,\sigma)$ is partitioned into four parts [1],

$$M_f(s,\sigma) = M_-(s,\sigma) + M_b(s,\sigma) + M_\infty(s,\sigma) + M_e(s,\sigma), \tag{12}$$

where

$$M_-(s,\sigma) = \sum_{i=1}^{n_a^-} \frac{R_i^-(\sigma)}{s-\lambda_i^-(\sigma)}, \quad M_b(s,\sigma) = \sum_{i=1}^{n_b} \frac{R_i^b(\sigma)}{s-\lambda_i^b(\sigma)}$$

and

$$M_\infty(s,\sigma) = \sum_{i=1}^{n_f} \frac{R_i^\infty(\sigma)}{s-\lambda_i^\infty(\sigma)}, \quad M_e(s,\sigma) = \sum_{i=1}^{n_e} \frac{R_i^e(\sigma)}{s-\lambda_i^e(\sigma)}.$$

According to the above partitions of $M_f(s,\sigma)$, we define the corresponding subsets of eigenvalues, right- and left-eigenvectors of $A_o(\sigma)$,

$$\Lambda_-(\sigma) := \{\lambda_i^- \mid i = 1,\cdots,n_a^-\}, \quad \Lambda_b(\sigma) := \{\lambda_i^b \mid i = 1,\cdots,n_b\},$$

$$\Lambda_\infty(\sigma) := \{\lambda_i^\infty \mid i = 1,\cdots,n_f\}, \quad \Lambda_e(\sigma) := \{\lambda_i^e \mid i = 1,\cdots,n_e\},$$

$$V_-(\sigma) := \{V_i^- \mid i = 1,\cdots,n_a^-\}, \quad V_b(\sigma) := \{V_i^b \mid i = 1,\cdots,n_b\},$$

$$V_\infty(\sigma) := \{V_i^\infty \mid i = 1,\cdots,n_f\}, \quad V_e(\sigma) := \{V_i^e \mid i = 1,\cdots,n_e\},$$

$$W_-(\sigma) := \{W_i^- \mid i = 1,\cdots,n_a^-\}, \quad W_b(\sigma) := \{W_i^b \mid i = 1,\cdots,n_b\},$$

$$W_\infty(\sigma) := \{W_i^\infty \mid i = 1,\cdots,n_f\}, \quad W_e(\sigma) := \{W_i^e \mid i = 1,\cdots,n_e\}.$$

Hereafter, we will use an over bar on a certain variable to denote its limit as $\sigma \to \infty$ whenever it exists. For example, $\overline{M}_e(s)$ and $\overline{W}_e$ denote respectively the limits of $M_e(s,\sigma)$ and $W_e(\sigma)$ as $\sigma \to \infty$.

From [1], we showed that irrespective of the target closed-loop transfer function $T_{zw}(s)$, both $M_-(s,\sigma)$ and $M_b(s,\sigma)$ can be rendered zero either exactly or asymptotically as $\sigma \to \infty$ by an appropriate finite eigenstructure assignment of A_o. Also, $M_\infty(s,\sigma)$ can be rendered asymptotically zero as $\sigma \to \infty$ by an appropriate asymptotically infinite eigenstructure assignment of A_o. On the other hand, in general, $M_e(s,\sigma)$ can never be rendered zero although there exists abundant amount of freedom to shape $M_e(s,\sigma)$ within the given constraints. However, when specialized to a particular class of target closed-loop transfer functions, namely $T_{zw}(s) \in \mathbf{T}^f_{\text{ER}}(\Sigma)$, $M_e(s,\sigma)$ can be rendered zero exactly. Similarly, $M_e(s,\sigma)$ can be rendered zero asymptotically as $\sigma \to \infty$ if $T_{zw}(s) \in \mathbf{T}^f_{\text{R}}(\Sigma)$.

Next, we describe in details the design constraints and the available design freedom on the observer gain matrix K in the eigenstructure assignment of A_o for closed-loop transfer recovery. The discussion covers each of the partitions of $M_f(s,\sigma)$ given in equation (12).

(a) $M_-(s,\sigma)$ partition: For an arbitrary target closed-loop transfer function $T_{zw}(s)$, the term $M_-(s,\sigma)$ can be made identically zero (irrespective of the value of σ). To accomplish this, the set of n_a^- eigenvalues in $\Lambda_-(\sigma)$ and the corresponding set of left-eigenvectors $V_-(\sigma)$ of A_o must be selected to coincide respectively with the set of stable invariant zeros and their corresponding left-state zero directions of Σ_{yw}. It is also possible to render $M_-(s,\sigma)$ zero asymptotically as $\sigma \to \infty$. This is done by parameterizing $\Lambda_-(\sigma)$ and the corresponding set of left-eigenvectors $V_-(\sigma)$ of A_o so that in the limit $\overline{\Lambda}_-$ and $\overline{V}_-$ coincide respectively with the set of stable invariant zeros and their corresponding left-state zero directions of Σ_{yw}.

(b) $M_b(s,\sigma)$ partition : For an arbitrary target closed-loop transfer function $T_{zw}(s)$, the term $M_b(s,\sigma)$ can be rendered identically zero (irrespective of the value of σ). To accomplish this, the set of n_b eigenvalues in $\Lambda_b(\sigma)$ can be assigned arbitrarily to any asymptotically finite or infinite locations in $\mathcal{C}^-$, while the corresponding set of left eigenvectors $V_b(\sigma)$ of A_o is constrained to

be in the null space of the matrix $[B_1 - K(\sigma)D_{21}]'$. Likewise, $M_b(s,\sigma)$ can be rendered asymptotically zero as $\sigma \to \infty$. This can be done by selecting an arbitrary set of $\Lambda_b(\sigma)$ from either asymptotically finite or infinite locations in $\mathcal{C}^-$, while the corresponding set of left eigenvectors $V_b(\sigma)$ of A_o is chosen such that in the limit $\overline{V}_b$ is in the null space of the matrix $[B_1 - K(\sigma)D_{21}]'$. Note that, in practice, one should keep elements of $\overline{\Lambda}_b$ at finite locations in order to reduce the need for a high-bandwidth controller.

(c) $M_\infty(s,\sigma)$ partition : For an arbitrary target closed-loop transfer function $T_{zw}(s)$, the term $M_\infty(s,\sigma)$ can be rendered asymptotically zero as $\sigma \to \infty$. The set of n_f eigenvalues in $\Lambda_\infty(\sigma)$ can be assigned to any asymptotically infinite locations in $\mathcal{C}^-$. That is, there exists a complete freedom in the way the eigenvalue $\lambda_i^\infty(\sigma) \in \Lambda_\infty(\sigma)$ tends to infinity as $\sigma \to \infty$, i.e. the asymptotic direction and the rate at which each $\lambda_i^\infty(\sigma)$ goes to infinity can be chosen freely by the designer. However, for every $\lambda_i^\infty(\sigma) \in \Lambda_\infty(\sigma)$, the corresponding right and left eigenvectors $W_i^\infty(\sigma)$ and $V_i^\infty(\sigma)$ must be such that $W_i^\infty(\sigma)[V_i^\infty(\sigma)]^H[B_1 - K(\sigma)D_{21}]$ is uniformly bounded as $\sigma \to \infty$. This constraint ensures that the residue $R_i^\infty(\sigma)$ remains uniformly bounded as $\sigma \to \infty$ and thereby forces $\overline{M}_\infty(s)$ to be zero.

(d) $M_e(s,\sigma)$ partition: The term $M_e(s,\sigma)$ does not exist when $n_a^+ + n_c = 0$, i.e. when the system Σ_{yw} is of minimum phase and left-invertible. For the case where $n_a^+ + n_c \neq 0$, we examine *first* the problem of an arbitrary target closed-loop transfer function $T_{zw}(s)$. Here, the term $M_e(s,\sigma)$ can never be rendered zero although there exists abundant amount of freedom to assign the associated eigenvalues and eigenvectors. To be explicit, the set of $n_a^+ + n_c$ eigenvalues in $\Lambda_e(\sigma)$ can be assigned to any (either asymptotically finite or infinite) locations in $\mathcal{C}^-$, with the provision that any unobservable (and stable since the pair (A, C_2) is assumed to be detectable) eigenvalues of Σ_{yw} be included in the set $\Lambda_e(\sigma)$. Also, there exists a complete freedom consistent with

the results of [7] in assigning the right- and left-eigenvector sets $W_e(\sigma)$ and $V_e(\sigma)$ and hence $\overline{W}_e$ and $\overline{V}_e$. But in general $\overline{\Lambda}_e$, $\overline{W}_e$ and $\overline{V}_e$ cannot be assigned such that $\overline{M}_e(s)$ is zero. However, there exists a multitude of ways to assign $\overline{\Lambda}_e$ and $\overline{W}_e$ (and hence $\overline{V}_e$). One possibility is to shape $\overline{M}_e(s)$ to have certain desired directional properties, or to try to make it as small as possible using some optimization techniques.

The above discussion on $M_e(s,\sigma)$ assumes that the target closed-loop transfer function $T_{zw}(s)$ is arbitrary. Apparently, one may be able to acquire additional design freedom by taking into account some structural properties of the full-state feedback gain matrix F. For example, as stated in theorem 5 of Part 1 [1], under the assumption that the system Σ_{zu} is left-invertible, then any admissible target closed-loop transfer function is recoverable (i.e. an element of $\mathbf{T}_{\mathrm{R}}^{f}(\Sigma)$) if and only if $\mathcal{V}^{+}(A, B_1, C_2, D_{21}) \subseteq Ker(F)$. Since $\mathcal{V}^{+}(A, B_1, C_2, D_{21})$ is the span of $\tilde{x}_a^{+} \oplus \tilde{x}_c$, a given $T_{zw}(s)$ is recoverable if and only if the state-feedback gain matrix F is of the form,

$$\Gamma_3^{-1} F \Gamma_1 = \begin{bmatrix} F_{a1}^{-} & 0 & F_{b1} & 0 & F_{f1} \\ F_{a2}^{-} & 0 & F_{b2} & 0 & F_{f2} \end{bmatrix} \tag{13}$$

where Γ_3 and Γ_1 are nonsingular transformation matrices defined in theorem 1 of [1] for the system Σ_{yw}. Thus, whenever $T_{zw}(s)$ is an element of $\mathbf{T}_{\mathrm{R}}^{f}(\Sigma)$, it can be easily shown from the special structure of F in (13) that the term $\overline{M}_e(s)$ is identically zero, irrespective of the way we pick the set of $n_a^{+} + n_c$ eigenvalues in $\Lambda_e(\sigma)$ and the associated right- and left-eigenvector sets $W_e(\sigma)$ and $V_e(\sigma)$. Similarly, as stated in theorem 3 of Part 1 [1] and again under the assumption that Σ_{zu} is left-invertible, then any admissible target closed-loop transfer function is exactly recoverable (i.e. an element of $\mathbf{T}_{\mathrm{ER}}^{f}(\Sigma)$) if and only if $\mathcal{S}^{-}(A, B_1, C_2, D_{21}) \subseteq \mathrm{Ker}(F)$. Since $\mathcal{S}^{-}(A, B_1, C_2, D_{21})$ is the span of $\tilde{x}_a^{+} \oplus \tilde{x}_c \oplus \tilde{x}_f$, the closed-loop transfer function $T_{zw}(s)$ is exactly recoverable if and only if F is of the form,

$$\Gamma_3^{-1} F \Gamma_1 = \begin{bmatrix} F_{a1}^{-} & 0 & F_{b1} & 0 & 0 \\ F_{a2}^{-} & 0 & F_{b2} & 0 & 0 \end{bmatrix}. \tag{14}$$

Now, whenever $T_{zw}(s)$ is an element of $\mathbf{T}_{\mathrm{ER}}^{f}(\Sigma)$, then from the special

structure of F given in (14), it can be shown that both $\overline{M}_e(s)$ and $\overline{M}_\infty(s)$ are zero, irrespective of the way we select the set of eigenvalues in $\Lambda_e(\sigma)$ and in $\Lambda_\infty(\sigma)$, and the associated set of eigenvectors $W_e(\sigma)$, $V_e(\sigma)$, $W_\infty(\sigma)$ and $V_\infty(\sigma)$. In fact, in this case, all eigenvalues of A_o can be assigned to finite locations in $\mathcal{C}^-$. Moreover, since we do not have to address the eigen assignment problem associated with asymptotically infinite eigenvalues, we no longer need to parameterize the observer gain K in terms of a tuning parameter σ.

III. DESIGN VIA 'ATEA'

The previous section summarizes the available design freedom as well as constraints associated with the problem of assigning the eigenstructure of observer dynamic matrix for closed-loop transfer recovery. We develop here a design procedure which follows the concept of asymptotic time-scale and eigenstructure assignment (ATEA) proposed originally in [12]. This concept has been successfully used to design full-order observers in the problem of loop transfer recovery for left-invertible and minimum-phase plants in [13], and for general strictly proper systems in [9]. In what follows, we will present a step-by-step ATEA design algorithm for general non-strictly proper systems. At first in subsection III.A, we give a design procedure for an arbitrary target closed-loop transfer function, i.e. without taking into account any specific characteristics of F. This is the most general design procedure. When a given $T_{zw}(s)$ is asymptotically recoverable, the state-feedback gain matrix F has the structure given in (13); this translates into additional freedom for selecting eigenvalues and eigenvectors of A_o. The procedure described in subsection III.A will yield a design that recovers $T_{zw}(s)$ only in the asymptotic sense. However, when exact recovery is possible, F has the structure given in (14) and in this case one can solve the ECLTR design problem with simply a finite eigenstructure assignment to A_o. For this case, the general ATEA design procedure of subsection III.A is greatly simplified and a design solution is presented in subsection III.B.

A. ACLTR Design Via ATEA

The ATEA design method is decentralized in nature. The original system is decomposed into several subsystems that can be addressed separately in the design for closed-loop transfer recovery. Basic underlying idea behind this method starts by expressing the system into the special coordinate basis (s.c.b) of Σ_{yw} (see theorem 1 of Part 1 [1] and also [10] and [11]). The finite eigenstructure of A_o is assigned by working with subsystems which represent the finite-zero structure of Σ_{yw} (cf. equations (8) and (9) of Part 1). Similarly, the asymptotically infinite eigenstructure of A_o is assigned by working with subsystems which represent the infinite-zero structure of Σ_{yw} (see equation (13) of Part 1 for each $i = 1$ to m_f).

There are two issues in formulating the observer-dynamic matrix $A_o = A - K(\sigma)C_2$ through the selection of $K(\sigma)$. The first one is related to eigenvalue assignment while the second one deals with eigenvector assignment. Let us first consider the problem of eigenvalue assignment. As discussed in section II, some eigenvalues of A_o are constrained while others can be freely assigned to any asymptotically finite or infinite locations in $\mathcal{C}^-$. To be specific,

(1) $\Lambda_-(\sigma)$ must coincide either exactly or in the asymptotic sense to the set of stable invariant zeros of Σ_{yw},

(2) $\Lambda_b(\sigma)$ and $\Lambda_e(\sigma)$ can be assigned freely to any asymptotically finite or infinite locations in $\mathcal{C}^-$ and,

(3) $\Lambda_\infty(\sigma)$ can only be assigned to asymptotically infinite locations in $\mathcal{C}^-$.

In order to conserve the controller bandwidth, both $\Lambda_b(\sigma)$ and $\Lambda_e(\sigma)$ should in practice be assigned to asymptotically finite locations. Let us next examine carefully the freedom available in assigning $\Lambda_\infty(\sigma)$. Clearly from the discussion in section II, a complete freedom is available in choosing each $\lambda_i^\infty(\sigma) \in \Lambda_\infty(\sigma)$ $(i = 1, \cdots, n_f)$. That is, both the asymptotic direction and the rate at which $\lambda_i^\infty(\sigma)$ goes to infinity can be set arbitrarily. In other words, the freedom available in assigning every asymptotically infinite eigenvalue $\lambda_i^\infty(\sigma)$ manifests itself in two

ways:

(1) First, we choose the asymptotic directions along which these eigenvalues tend to infinity and,

(2) Secondly, we select the rates at which they tend to infinity.

To quantify both these choices, let $\Lambda_\infty(\sigma)$ for large values of σ be subdivided into r sets where $r \leq n_f$,

$$\frac{\Lambda_1}{\mu_1}, \frac{\Lambda_2}{\mu_2}, \cdots, \frac{\Lambda_r}{\mu_r}. \tag{15}$$

Here, $\Lambda_\ell(\ell = 1, \cdots, r)$ is a set of n_ℓ numbers in $\mathcal{C}^-$ and Λ_ℓ is closed under complex conjugation. Also $\sum_{\ell=1}^{r} n_\ell = n_f$. Apparently, the elements of Λ_ℓ define the asymptotic directions of the infinitely fast eigenvalues while the small parameters μ_ℓ $(\ell = 1, \cdots, r)$ which are a function of σ define the rates at which these eigenvalues tend to infinity.

In summary, regarding the eigenvalue assignment, we have the freedom to specify

(i) the asymptotic limits $\overline{\Lambda}_b$ and $\overline{\Lambda}_e$ of $\Lambda_b(\sigma)$ and $\Lambda_e(\sigma)$ and,

(ii) Λ_ℓ and μ_ℓ $(\ell = 1, \cdots, r)$.

Note that $\overline{\Lambda}_b$ and $\overline{\Lambda}_e$ together with $\overline{\Lambda}_-$ define all the asymptotically finite eigenvalues of A_o, while Λ_ℓ and μ_ℓ $(\ell = 1, \cdots, r)$ define the remaining asymptotically infinite eigenvalues.

Let us look now at the constraints and design freedom available in assigning the eigenvectors of A_o. The set of left-eigenvectors $\overline{V}_-$ is constrained to coincide with the corresponding set of left state-zero directions of the plant. Moreover, $Im\overline{V}_-$ coincides the subspace

$$\mathcal{V}^*(A, B_1, C_2, D_{21})/\mathcal{V}^+(A, B_1, C_2, D_{21}).$$

On the other hand, the set of eigenvectors $\overline{V}_b$ is constrained to be in the null space of $[B_1 - K(\sigma)D_{21}]'$. In view of the particular structure of s.c.b, it can be seen that every element $\overline{V}_i^b$ of $\overline{V}_b$ is constrained to be of the form

$$[0,\ 0,\ (V_i^b)^H,\ 0,\ 0]^H.$$

In other words, the set $\overline{V}_b$ can be represented in a matrix notation as

$$[0,\ 0,\ (V_b^b)^H,\ 0,\ 0]^H$$

where V_b^b is a $n_b \times n_b$ matrix. Thus the selection of $\overline{V}_b$ to be in the null space of $[B_1 - K(\sigma)D_{21}]'$ is equivalent to an arbitrary selection of V_b^b consistent with the freedom available for eigenvector assignment [7]. Again in view of the properties of s.c.b, we note that the columns of $\overline{V}_b$ span the subspace

$$\Re^n / \{\mathcal{S}^+(A, B_1, C_2, D_{21}) \cup \mathcal{S}^-(A, B_1, C_2, D_{21})\}.$$

There is also freedom available in specifying $\overline{W}_e$. It is shown in [4] that $Im\overline{W}_e$ coincides with the subspace $\mathcal{V}^+(A, B_1, C_2, D_{21})$. Again due to the special structure of s.c.b, $\overline{W}_e$ has the special matrix form

$$[(W_e^+)^H,\ 0,\ 0,\ (W_e^c)^H,\ 0]^H$$

where $W_{ee} \equiv [(W_e^+)^H,\ (W_e^c)^H]^H$ is a $n_e \times n_e$ matrix. Thus, an appropriate selection of $\overline{W}_e$ is equivalent to an arbitrary selection of W_{ee} consistent with the freedom available for eigenvector assignment [7].

Now, an assignment of both asymptotically finite and infinite eigenvalues and the corresponding eigenvectors to A_o can be viewed as a problem in asymptotic time-scale and eigenstructure assignment (ATEA). Further discussion on time-scale structure of a system can be found in [9]. In order to have a well-defined separation of time scales, we will assume throughout the paper that

$$\mu_\ell / \mu_{\ell+1} \to 0 \text{ as } \mu_{\ell+1} \to 0. \tag{16}$$

We emphasize that the freedom available in the asymptotically infinite eigenstructure of A_o is captured in the selection of an appropriate fast time-scale structure. The asymptotic directions of asymptotically infinite eigenvalues are specified in the sets Λ_ℓ $(\ell = 1, \cdots, r)$ and $r \leq n_f$. Different values of time scales are defined by the small positive parameters μ_ℓ $(\ell = 1, \cdots, r)$, which are function of a tuning parameter σ so that (16) holds as $\sigma \to \infty$. Note that there is another constraint on the

infinite eigenstructure; namely for every asymptotically infinite eigenvalue $\lambda_i^\infty(\sigma)$, the corresponding right- and left-eigenvectors $W_i^\infty(\sigma)$ and $V_i^\infty(\sigma)$ of A_o must be such that

$$W_i^\infty(\sigma)[V_i^\infty(\sigma)]^H[B_1 - K(\sigma)D_{21}]$$

remains uniformly bounded as $\sigma \to \infty$. This constraint is automatically satisfied using the ATEA design procedure described in this section.

In what follows, we give a step-by-step design algorithm for ATEA. In view of the above discussion, input parameters to the algorithm are $\overline{\Lambda}_b$, V_b^b, $\overline{\Lambda}_e$, W_{ee}, Λ_ℓ and μ_ℓ ($\ell = 1, \cdots, r$), as well as the integer r. Among these, the primary ones are:

(1) $\overline{\Lambda}_e$ and W_{ee} which shape the error term $\overline{M}_e(s)$ and,

(2) Λ_ℓ and μ_ℓ ($\ell = 1, \cdots, r$), which define the time-scale structure of the observer and thus have a strong impact on the size of the resulting controller gain.

The remaining input parameters, namely $\overline{\Lambda}_b$ and V_b^b, are considered as secondary inputs.

The ATEA design algorithm can be divided into three steps. Steps 1 and 2 work with design at individual subsystem levels for the assignment of the asymptotically finite and infinite eigenstructures respectively. In step 3, designs at each subsystem level in steps 1 and 2 are then put together to form a complete design for closed-loop transfer recovery.

Step 1 : This step deals with the assignment of asymptotically finite eigenstructure (i.e., slow time-scale structure) and makes use of subsystems (8) to (11) of Part 1. $\lambda(A_{aa}^-)$ are the stable invariant zeros of Σ_{yw} and they form eigenvalues of A_o in the set $\overline{\Lambda}_-$, while the corresponding left-eigenvectors of A_o coincide with the left state-zero directions of Σ_{yw}. To place the set of eigenvalues $\overline{\Lambda}_b$ and left-eigenvectors $\overline{V}_b$, we choose a gain K_b such that $\lambda(A_{bb}^c)$ coincides with $\overline{\Lambda}_b$ while V_b^b coincides with the set of left-eigenvectors of A_{bb}^c where

$$A_{bb}^c = A_{bb} - K_b C_b. \tag{17}$$

Note that existence of such a K_b is guaranteed by the property 2 of

section III in Part 1 [1] and as long as the eigenvector set $\overline{V}_b$ is consistent with the freedom available in the eigenvector assignment [7]. Next, in order to place the set of eigenvalues $\overline{\Lambda}_e$ and right-eigenvectors W_{ee}, let us first form the matrices A_{ee} and C_e as follows,

$$A_{ee} = \begin{bmatrix} A_{aa}^{+} & 0 \\ B_c E_{ca}^{+} & A_{cc} \end{bmatrix}, \quad C_e = \begin{bmatrix} C_{e0} \\ C_{e1} \end{bmatrix} = \begin{bmatrix} C_{0a}^{+} & C_{0c} \\ E_a^{+} & E_c \end{bmatrix}, \tag{18}$$

where

$$E_a^{+} = [(E_{1a}^{+})', (E_{2a}^{+})', \ldots, (E_{m_f a}^{+})']',$$

$$E_{ia} = [E_{ia}^{+}, E_{ia}^{-}], \quad E_c = [E_{1c}', E_{2c}', \ldots, E_{m_f c}']'.$$

Now, a gain $K_e = [K_{e0}, K_{e1}]$ can be chosen such that the set of eigenvalues and right-eigenvectors of A_{ee}^{c} coincide with $\overline{\Lambda}_e$ and W_{ee} respectively where

$$A_{ee}^{c} = A_{ee} - K_e C_e = A_{ee} - K_{e0} C_{e0} - K_{e1} C_{e1}. \tag{19}$$

Again, note that existence of such a K_e is guaranteed by the property 2 of section III of [1] and as long as the eigenvector set W_{ee} is consistent with the freedom available in the eigenvector assignment [7]. For future use, let us define

$$A_{ee1} = A_{ee} - K_{e0} C_{e0}, \quad K_{e0} = \begin{bmatrix} K_{a0}^{+} \\ K_{c0} \end{bmatrix},$$

and partition K_{e1} as

$$K_{e1} = [\, K_{e11}, \quad K_{e12}, \quad \cdots, \quad K_{e1 m_f} \,] \tag{20}$$

where K_{e1i} is a vector of dimension $n_e \times 1$.

Step 2 : Here, we deal with the assignment of asymptotically infinite eigenstructure (i.e. the fast time-scale structure) and apply it to m_f subsystems represented by (13) of Part 1. This step is only needed when $n_f > 0$. As discussed earlier, a complete freedom is available to specify any number r ($r \leq n_f$) of fast time scales. The simplest case is to choose $r = 1$. However, for generality, we consider the case where $r > 1$. Assignment of the fast time scales is done through selection of the set Λ_ℓ and the corresponding positive parameters μ_ℓ ($\ell = 1, \cdots, r$).

The procedure for assigning the fast time-scale eigenstructure is again accomplished in a decentralized fashion. We consider the eigenassignment problem for each i-th single-input single-output subsystem ($i = 1, \cdots, m_f$) separately. Thus, we need to distribute elements of the specified sets Λ_ℓ and the parameters μ_ℓ ($\ell = 1, \cdots, r$) to each of the m_f subsystems. The distribution can be done in a number of ways. Let the subsystem i be assigned r_i different time scales for some $r_i \leq q_i$ and Λ_{ij}/μ_{ij} ($1 \leq j \leq r_i$) be the asymptotically infinite eigenvalues assigned to the subsystem i. Define n_{ij} to be the number of eigenvalues corresponding to the time scale t/μ_{ij}. That is, the set Λ_{ij} contains n_{ij} elements. As usual, the set Λ_{ij} is assumed to be closed under complex conjugation. Also, in order to have a set of well separated time scales in the subsystem i, we assume that

$$\mu_{ij}/\mu_{ij+1} \to 0 \text{ as } \mu_{ij+1} \to 0 \text{ for all } j \ (1 \leq j \leq r_i - 1). \tag{21}$$

Obviously when $r = 1$, we have applied a single time scale to all subsystems , i.e all μ_{ij} are equal to a single parameter μ and all r_i are equal to unity. In this case, the tuning parameter σ can be taken as $1/\mu$. With these preliminaries, we are now ready to design for the i-th subsystem. At first, we will find a gain matrix K_{ij} for each time-scale t/μ_{ij} ($1 \leq j \leq r_i$). For this subsystem, we define a matrix G_{ij} of dimension $n_{ij} \times n_{ij}$ and a matrix C_{ij} of dimension $1 \times n_{ij}$ with the following structure,

$$G_{ij} = \begin{bmatrix} 0 & I_{n_{ij}-1} \\ 0 & 0 \end{bmatrix} \text{ and } C_{ij} = \begin{bmatrix} 1 & 0 \end{bmatrix}.$$

An eigenvalue assignment on this subsystem is done using a gain vector K_{ij} of dimension $n_{ij} \times 1$ such that the eigenvalues of G_{ij}^c coincide with Λ_{ij} where $G_{ij}^c = G_{ij} - K_{ij}C_{ij}$. It is clear that one can always find such a matrix K_{ij} since the pair (G_{ij}, C_{ij}) defined above is observable. Let's further partition the matrix K_{ij} as

$$K_{ij} = \begin{bmatrix} K_{ijc} \\ K_{ijd} \end{bmatrix}$$

where the last element K_{ijd} is a scalar. Moreover, since the subsystem matrix G_{ij}^c is stable, the gain K_{ijd} must also be nonzero. Next, the

gains K_{ij} $(1 \le j \le r_i)$ obtained above are put together to form a gain vector that gives the desired fast time scales in the i-th subsystem. In the process, we parameterize the design solution as a function of a tuning parameter σ. For the description of this part of the ATEA design procedure, let us define the following scalars,

$$J_{i1} = 1 \ , \ J_{ij} = \prod_{\ell=1}^{j-1} K_{i\ell d} \ , \ (2 \le j \le r_i).$$

and

$$\alpha_{i0} = 0 \ , \ \alpha_{ij} = \sum_{k=1}^{j} n_{ik} \ , \ (1 \le j \le r_i).$$

Note that $\alpha_{ir_i} = q_i$. Also, for each j $(1 \le j \le r_i)$,

$$\epsilon_{i\alpha_{ij-1}+1} = \epsilon_{i\alpha_{ij-1}+2} = \cdots = \epsilon_{i\alpha_{ij-1}+n_{ij}} = \mu_{ij}$$

and

$$\eta_i = \prod_{k=1}^{q_i} \epsilon_{ik}. \tag{22}$$

Now, we are ready to give the design gain $\tilde{K}_i(\sigma)$ for the subsystem i parameterized by a variable σ as follows,

$$\tilde{K}_i(\sigma) = \left[\tilde{K}'_{i1}(\sigma), \ \tilde{K}'_{i2}(\sigma), \ \cdots, \ \tilde{K}'_{ir_i}(\sigma)\right]' \tag{23}$$

where

$$\tilde{K}_{ij}(\sigma) = \frac{1}{\eta_i} J_{ij} S_{ij} K_{ij}.$$

and

$$S_{ij} = \text{Diag}\left[\prod_{\ell=\alpha_{ij-1}+2}^{q_i} \epsilon_{i\ell} \ , \ \prod_{\ell=\alpha_{ij-1}+3}^{q_i} \epsilon_{i\ell} \ , \ \cdots \ , \ \prod_{\ell=\alpha_{ij-1}+n_{ij}}^{q_i} \epsilon_{i\ell}\right]. \tag{24}$$

The product $\prod_{\ell=\alpha_{ij-1}+n_{ij}}^{q_i} \epsilon_{i\ell}$ in (24) is taken to be unity when $j = r_i$. The above design formulation becomes much simpler when $r_i = 1$. For this case, let $\overline{\mu}_i$ denote the time-scale parameter, then

$$\tilde{K}_i(\sigma) = \frac{1}{(\overline{\mu}_i)^{q_i}} \left[(\overline{\mu}_i)^{q_i-1} K_{i1}, \ (\overline{\mu}_i)^{q_i-2} K_{i2}, \ \cdots, \ K_{iq_i}\right]' \tag{25}$$

where the individual gains $K_{ij}(1 \leq j \leq q_i)$ have been previously selected such that the eigenvalues of G_i^c are placed at the desired locations and

$$G_i^c = -\begin{bmatrix} K_{i1}, & K_{i2}, \cdots, & K_{iq_i-1} & K_{iq_i} \\ & -I_{q_i-1} & & 0 \end{bmatrix}'.$$

Here we did not discuss any eigenvector assignment. However, it turns out that our eventual design is such that the eigenvectors corresponding to the asymptotically infinite eigenvalues are naturally assigned to appropriate locations so that $M_\infty(j\omega, \sigma) \to 0$ as $\sigma \to \infty$.

Step 3 : This constitutes the last step in the ATEA design procedure. Here, various gains obtained in steps 1 and 2 are combined to form an overall observer gain for the system Σ_{yw} parameterized by a tuning parameter σ. Let's define the gain matrix $\tilde{K}_{e1}$ as

$$\tilde{K}_{e1}(\sigma) = \begin{bmatrix} \tilde{K}_{a1}^+(\sigma) \\ \tilde{K}_{c1}(\sigma) \end{bmatrix} = \left[\tilde{K}_{e11}(\sigma),\ \tilde{K}_{e12}(\sigma),\ \cdots,\ \tilde{K}_{e1m_f}(\sigma)\right],$$

$$\tilde{K}_{e1i}(\sigma) = \frac{1}{\eta_i} J_{ir_i} K_{ir_id} K_{e1i}. \tag{26}$$

Note that when $r_i = 1$, the gain K_{i1d} is the same as K_{iq_i} and η_i is the same as $(\overline{\mu}_i)^{q_i}$. For the case where $n_f > 0$, the observer gain $K(\sigma)$ adjustable by a single tuning parameter σ is given by

$$K(\sigma) = \Gamma_1 \tilde{K}(\sigma) \Gamma_2^{-1} \tag{27}$$

where

$$\tilde{K}(\sigma) = \begin{bmatrix} B_{0a}^- & L_{af}^- + \tilde{H}_{af}^- & L_{ab}^- + \tilde{H}_{ab}^- \\ B_{0a}^+ + K_{a0}^+ & L_{af}^+ + \tilde{H}_{af}^+ + \tilde{K}_{a1}^+(\sigma) & L_{ab}^+ + \tilde{H}_{ab}^+ \\ B_{0b} & L_{bf} + \tilde{H}_{bf} & K_b \\ B_{0c} + K_{c0} & L_{cf} + \tilde{H}_{cf} + \tilde{K}_{c1}(\sigma) & L_{cb} + \tilde{H}_{cb} \\ B_{0f} & L_f + \tilde{K}_f(\sigma) & 0 \end{bmatrix} \tag{28}$$

and

$$\tilde{K}_f(\sigma) = \text{Diag}\left[\tilde{K}_1(\sigma),\ \tilde{K}_2(\sigma),\ \cdots, \tilde{K}_{m_f}(\sigma)\right],$$

$$L_f = \left[L_1',\ L_2',\ \cdots, L_{m_f}'\right]'$$

Note that the matrices $\tilde{H}_{af}^{+}$, $\tilde{H}_{ab}^{+}$, $\tilde{H}_{af}^{-}$, $\tilde{H}_{ab}^{-}$, $\tilde{H}_{bf}$, $\tilde{H}_{cf}$ and $\tilde{H}_{cb}$ are arbitrary but finite and used to introduce additional design freedom. We can now state the following theorem.

Theorem 1. *Consider a full-order observer-based controller with gain matrix given by (27) and assume that $n_f > 0$. Then, we have the following properties:*

1. *There exists a scalar σ^* such that, for all $\sigma > \sigma^*$, the observer design is asymptotically stable. Furthermore, the observer dynamic matrix has the following time-scale structures: t, t/μ_{ij} (where $j = 1, \cdots, r_i$ and $i = 1, \cdots, m_f$). That is, its eigenvalues as $\mu_r \to 0$ are given by*

$$\overline{\Lambda}_- + 0(\mu_r)\ ,\ \overline{\Lambda}_b + 0(\mu_r)\ ,\ \overline{\Lambda}_e + 0(\mu_r)\ ,$$

$$\frac{\Lambda_{ij}}{\mu_{ij}} + 0(1) \quad \text{for} \quad (j = 1, \cdots, r_i) \quad \text{and} \quad (i = 1, \cdots, m_f).$$

   Moreover, if $\tilde{H}_{af}^{-} = 0$ and $\tilde{H}_{bf} = 0$, some finite eigenvalues of A_o are exactly equal to $\overline{\Lambda}_-$ and $\overline{\Lambda}_b$ for all σ rather than asymptotically tending to $\overline{\Lambda}_-$ and $\overline{\Lambda}_b$.

2. *CLTR is achieved in the sense that, as $\sigma \to \infty$, $M_f(s, \sigma) \to \overline{M}_e(s)$ pointwise in s.*

Proof : See [5]. ∎

Remark 1. *For the case when $n_f = 0$, observer gains obtained from the above ATEA procedure are independent of σ and are given by*

$$K(\sigma) = \Gamma_1 \begin{bmatrix} B_{0a}^{-} & L_{ab}^{-} \\ B_{0a}^{+} + K_{a0}^{+} & L_{ab}^{+} \\ B_{0b} & K_b \\ B_{0c} + K_{c0} & L_{cb} \end{bmatrix} \Gamma_2^{-1}. \tag{29}$$

Furthermore, the eigenvalues of A_o are precisely those of $\overline{\Lambda}_- \cup \overline{\Lambda}_b \cup \overline{\Lambda}_e$ and $M_f(s, \sigma) = \overline{M}_e(s)$.

Remark 2. *When $T_{zw}(s)$ is an element of $\mathbf{T}_{\mathrm{R}}^{f}(\Sigma)$ and due to the special structure of F in (13), $\overline{M}_e(s)$ is identically zero irrespective of the way we select the set of $n_a^{+} + n_c$ eigenvalues in $\Lambda_e(\sigma)$ and the set of right- and left-eigenvectors $W_e(\sigma)$ and $V_e(\sigma)$.*

Clearly, the ATEA design method presented above has the attractive feature that it is decentralized. Different time scales and eigenstructures can be assigned to the subsystems of Σ_{yw} separately. The design in each subsystem does not require an explicit value of the tuning parameter σ. The variable σ enters only in (23) or (25) when designs for different subsystems are put together to form the final observer gain with the desired time-scale structure. The variable σ will act as a tuning parameter based on the chosen time scales for the fast observer dynamics.

B. ECLTR Design Via ATEA

In the previous subsection, we have presented ATEA design methodology and utilized it for ACLTR design. The power of this method is that it explores all the degrees of freedom available and provides at the end a family of parameterized controllers $\mathbf{C}(s, \sigma)$ to achieve closed-loop transfer recovery. Depending upon the particular design requirements, one would adjust the tuning parameter σ until a desired recovery is achieved. This asymptotic procedure is no longer needed when a given target closed-loop transfer function $T_{zw}(s)$ is exactly recoverable (i.e. $T_{zw}(s) \in \mathbf{T}^f_{\text{ER}}(\Sigma)$). As discussed in section II, when $T_{zw}(s) \in \mathbf{T}^f_{\text{ER}}(\Sigma)$, F has the form given in (14). With this particular structure of F, all eigenvalues of A_o can be assigned to finite locations and the above ATEA design procedure can be simplified drastically. In fact, the design requires only finite eigenstructure assignment and does not involve fast time-scale structure assignment. The intent of this section is to describe in detail the available design freedom and provide a step-by-step design procedure in the eigenstructure assignment of A_o for exact closed-loop transfer function recovery (ECLTR).

Note that for an exactly recoverable case, the observer gain K is no longer parameterized as a function of σ and thus, dependency of σ is dropped in the following discussion. Based on the different partitions of $M_f(s)$ in section II, the design freedom available for each subsystem is as follows,

1. A set of n_a^- eigenvalues of A_o in Λ_- must be chosen to coincide

exactly with the set of stable invariant zeros of the system Σ_{yw}. The corresponding left-eigenvectors of A_o must coincide exactly with the left state-zero directions of Σ_{yw} so that $M_-(s)$ is identically zero.

2. A set of n_b eigenvalues of A_o in Λ_b can be freely assigned to any finite locations in $\mathcal{C}^-$. Moreover, the set of eigenvectors V_b corresponding to these eigenvalues must be in the null space of $(B_1 - KD_{21})'$ and satisfying the constraints defined in [7]. The resulting $M_b(s)$ will be identically zero.

3. A set of $n_a^+ + n_c$ eigenvalues of A_o in Λ_e can be freely assigned to any finite locations in $\mathcal{C}^-$ subject to the condition that any unobservable eigenvalues of Σ_{yw} must be included in the set Λ_e. Moreover, the set of eigenvectors W_{ee} corresponding to these eigenvalues can be selected freely within the constraints defined in [7]. We note that due to the specific structure of F in (14), $M_e(s)$ is zero regardless of how we select Λ_e and W_{ee}. Note that this step is not needed when $n_a^+ + n_c = 0$, i.e when the system Σ_{yw} is of minimum phase and left-invertible.

4. A set of n_f eigenvalues of A_o in Λ_d can be freely assigned to any finite locations in $\mathcal{C}^-$. (The sets Λ_∞ and V_∞ are renamed as Λ_d and V_d to highlight the fact that these eigenvalues do not need to be at infinity for exact recovery). The set of eigenvectors V_d corresponding to these eigenvalues can be selected freely within the constraints defined in [7]. With F in the form of (14), the partition $M_\infty(s)$ is identically zero irrespective of how we select Λ_d and V_d.

We now proceed to the design of an observer gain K that produces the desired finite eigenstructure to A_o for the case of exact closed-loop recovery.

Step 1a : This step deals with the assignment of finite eigenstructure to the subsystem (10) of Part 1. We choose a gain K_b such that $\lambda(A_{bb}^c)$

coincides with Λ_b, a selected set of n_b eigenvalues in $\mathcal{C}^-$ where

$$A_{bb}^c = A_{bb} - K_b C_b. \tag{30}$$

Note that existence of such a K_b is guaranteed by the property 2 of section III of Part 1 [1]. The eigenvectors of A_{bb}^c can be freely assigned within the available freedom for eigenvector assignment [7]. Under the properties of s.c.b, the above ATEA design procedure always results in a set of eigenvectors V_b for the eigenvalues Λ_b of A_o that lie in the null space of $(B_1 - KD_{21})'$; hence rendering $M_b(s) = 0$.

Step 1b : This step deals with the assignment of finite eigenstructure to the subsystems (9), (11) and (13) of Part 1. Let the matrices A_x and C_x be defined as

$$A_x = \begin{bmatrix} A_{aa}^+ & 0 & L_{af}^+ C_f \\ B_c E_{ca}^+ & A_{cc} & L_{cf} C_f \\ B_f E_a^+ & B_f E_c & A_f \end{bmatrix}, \quad C_x = \begin{bmatrix} C_{0a}^+ & C_{0c} & C_{0f} \\ 0 & 0 & C_f \end{bmatrix}. \tag{31}$$

and $\Lambda_x \equiv \Lambda_e \cup \Lambda_d$ be a set of $n_a^+ + n_c + n_f$ eigenvalues in $\mathcal{C}^-$ which must include any unobservable eigenvalues of the system Σ_{yw}. Now, we select a gain K_x such that $\lambda(A_x^c)$ coincides with Λ_x where

$$A_x^c = A_x - K_x C_x. \tag{32}$$

Note that existence of such a K_x is guaranteed by the property 2 of section III of Part 1. The eigenvectors of A_x^c can be assigned within the freedom available for eigenvector assignment [7]. Let us partition the gain matrix K_x as follows,

$$K_x = \begin{bmatrix} K_{a0}^+ & K_{a1}^+ \\ K_{c0} & K_{c1} \\ K_{f0} & K_{f1} \end{bmatrix}.$$

Step 2 : Here, the gain matrices K_b and K_x obtained in step 1 are combined to give the desired observer gain for exact closed-loop transfer recovery. It is given by

$$K = \Gamma_1 \tilde{K} \Gamma_2^{-1} \tag{33}$$

where

$$\tilde{K} = \begin{bmatrix} B_{0a}^{-} & L_{af}^{-} & L_{ab}^{-} \\ B_{0a}^{+} + K_{a0}^{+} & K_{a1}^{+} & L_{ab}^{+} \\ B_{0b} & L_{bf} & K_b \\ B_{0c} + K_{c0} & K_{c1} & L_{cb} \\ B_{0f} + K_{f0} & K_{f1} & 0 \end{bmatrix}. \tag{34}$$

We have the following theorem.

Theorem 2. *Consider a full-order observer-based controller with a gain given by (33). Then, this full-order observer-based controller achieves CLTR and the eigenvalues of the resulting observer design are in the set* $\Lambda_- \cup \Lambda_b \cup \Lambda_x$.

Proof : See [5]. ∎

Remark 3. *In general, the observer gain for ECLTR is not unique.*

IV. OPTIMIZATION-BASED DESIGN METHODS

Clearly from section II, the whole notion of ACLTR is to make the recovery matrix

$$M_f(s) = F(sI_n - A + KC_2)^{-1}(B_1 - KD_{21})$$

as small as possible. The previously discussed design method ATEA accomplishes this task from the perspective of asymptotic time-scale and eigenstructure assignment to the observer dynamic matrix. An alternative method is to formulate the design problem in terms of finding a gain K that minimizes some norm (e.g. H_2 or H_∞) of $M_f(s)$. That is, one can cast the ACLTR design into an optimization problem. An optimal or suboptimal solution to such problem will provide the necessary observer design gain.

From this perspective, in this section, we will cast the closed-loop transfer recovery problem into a standard H_2- or H_∞- optimization problem. To begin, we consider the following auxiliary system,

$$\Sigma_a : \begin{cases} \dot{x} = A'x + C_2'u + F'w, \\ y = x, \\ z = B_1'x + D_{21}'u. \end{cases} \tag{35}$$

Here, w is modeled as an exogenous disturbance input to Σ_a and u is the control input. The variables y and z represent respectively the measured system states and the controlled outputs. If we consider a state-feedback law for the control u,

$$u = -K'x. \tag{36}$$

Then it is simple to verify that the closed-loop transfer function from w to z, denoted by $T_{zw}^{au}(s)$, is indeed equal to $M_f'(s)$. Now the ACLTR design problem can be casted into a problem of designing a state-feedback gain K' such that

(1) the auxiliary system Σ_a under the control law (36) is asymptotically stable and,

(2) the norm (H_2 or H_∞) of $M_f(s)$ is minimized.

There exists a vast literature on H_2 or H_∞ minimization methods. Borrowing from such a literature, subsection IV.A discusses algorithms for H_2 minimization of $M_f(s)$ while subsection IV.B does the same for H_∞ minimization. We want to emphasize that the optimization problem is cast here in terms of minimizing an appropriate norm of recovery matrix $M_f(s)$ rather than the actual recovery error $E(s)$.

It is well known that an optimal solution for either H_2 or H_∞ minimization of $M_f(s)$ does not necessarily exist, and the infimum of $\|M_f(s)\|_{H_2}$ or $\|M_f(s)\|_{H_\infty}$ is in general nonzero. However, for the class of exactly recoverable target closed-loop transfer functions $\mathbf{T}_{\text{ER}}^f(\Sigma)$, the infimum of $\|M_f(s)\|_{H_2}$ or $\|M_f(s)\|_{H_\infty}$ is in fact zero and it can be attained using a finite gain K. Also, for another class of target closed-loop transfer functions, namely the class of asymptotically recoverable target closed-loops $\mathbf{T}_{\text{AR}}^f(\Sigma)$, the infimum of $\|M_f(s)\|_{H_2}$ or $\|M_f(s)\|_{H_\infty}$ is also zero, and it can only be attained in an asymptotic sense by using larger and larger gain K. Whether the infimum of $\|M_f(s)\|_{H_2}$ or $\|M_f(s)\|_{H_\infty}$ is zero or not, the recovery procedure involves generating a sequence of gains with the property that in the limit H_2- or H_∞-norms of the recovery matrices approaches the infimum of $\|M_f(s)\|_{H_2}$ or $\|M_f(s)\|_{H_\infty}$ over the set of all possible gains. One normally settles with a suboptimal solution corresponding to a particular member of the sequence. In

H_2-optimization, an observer gain is generated via the solution of an algebraic Riccati equation (called hereafter H_2-ARE) parameterized in terms of a tuning parameter σ. A sequence of suboptimal gains is generated by letting σ tend to ∞. Similarly, if we let γ^* to be the infimum of $\|M_f(s)\|_{H_\infty}$ over the set of all possible gains, then for given a parameter γ greater than γ^*, one generates in H_∞-optimization a gain by solving an algebraic Riccati equation (called hereafter H_∞-ARE) parameterized in terms of γ so that the resulting $\|M_f(s,\gamma)\|_{H_\infty}$ is strictly less than γ. By gradually reducing γ, one thereby generates a sequence of suboptimal gains.

For simplicity and without loss of generality, we assume throughout this section that the matrix D_{21} is of the form,

$$D_{21} = \begin{bmatrix} I_{m_0} & 0 \\ 0 & 0 \end{bmatrix}.$$

Also, we partition the matrices B_1 and C_2 as

$$B_1 = [\, B_{1,0}, \quad B_{1,1}\,] \quad \text{and} \quad C_2 = \begin{bmatrix} C_{2,0} \\ C_{2,1} \end{bmatrix},$$

and let $A_1 = A - B_{1,0}C_{2,0}$. In the next two sections, we examine specific algorithms for the design of observer gain in the problem of CLTR using H_2 - and H_∞-optimization methods.

A. CLTR Design Via H_2-Optimization

In this subsection, we consider H_2-norm minimization of $M_f(s)$ or equivalently $T_{zw}^{au}(s)$. At first, let us look at an elegant way of computing the infimum value of $\|M_f(s)\|_{H_2}$ in a recent work by Stoorvogel [15]. We first recall the following lemma.

Lemma 1. *Assume that (A, C_2) is detectable. Then the infimum of $\|M_f(s)\|_{H_2}$ over all the stabilizing observer gains is given by*

$$Trace\{F\overline{P}F'\},$$

where $\overline{P} \in \Re^{n\times n}$ is the unique positive semi-definite matrix satisfying:

1. $F(\overline{P}) = \begin{bmatrix} A\overline{P} + \overline{P}A' + B_1B_1' & \overline{P}C_2' + B_1D_{21}' \\ C_2\overline{P} + D_{21}B_1' & D_{21}D_{21}' \end{bmatrix} \geq 0,$

2. $rank\, F(\overline{P}) = normrank\,\{C_2(sI_n - A)^{-1}B_1 + D_{21}\} \;\; \forall s \in \mathcal{C}^+/\mathcal{C}^o,$

3. $rank \begin{bmatrix} [sI - A', & -C_2'] \\ & F(\overline{P}) \end{bmatrix} = n + normrank\,\{C_2(sI_n - A)^{-1}B_1 + D_{21}\} \;\; \forall s \in \mathcal{C}^+/\mathcal{C}^o.$

Here normrank$\{\cdot\}$ denotes the rank of matrix $\{\cdot\}$ over the field of rational functions.

Proof : See Stoorvogel [15]. ∎

In general, as discussed earlier, the infimum of $\|M_f(s)\|_{H_2}$ can only be obtained asymptotically. In what follows, we give an algorithm that produces a sequence of parameterized observer gains $K(\sigma)$ for the general system Σ_a such that the H_2-norm of the recovery matrix, which is also parameterized by σ and is denoted by $M_f'(s,\sigma) = T_{zw}^{au}(s,\sigma)$, tends to the infimum of $\|M_f(s)\|_{H_2}$ as $\sigma \to \infty$. The algorithm consists of the following two steps:

Step 1 : Solve the following parameterized algebraic Riccati equation (H_2-ARE) for a given value of σ,

$$A_1\tilde{P} + \tilde{P}A_1' - \tilde{P}C_{2,0}'C_{2,0}\tilde{P} - \sigma\tilde{P}C_{2,1}'C_{2,1}\tilde{P} + B_{1,1}B_{1,1}' + \frac{1}{\sigma}I_n = 0, \quad (37)$$

for a positive definite solution $\tilde{P}$. We note that a unique positive definite solution $\tilde{P}$ of (37) always exists for all $\sigma > 0$. Obviously, $\tilde{P}$ is a function of σ and is denoted by $\tilde{P}(\sigma)$.

Step 2 : Let

$$K(\sigma) = [B_{1,0} + \tilde{P}(\sigma)C_{2,0}', \; \sigma\tilde{P}(\sigma)C_{2,1}']. \quad (38)$$

We have the following theorem.

Theorem 3. *Consider a full-order observer-based controller with a gain given in (38) and let $M_f(s,\sigma)$ be the resulting recovery matrix.*

Then, we have

$$\lim_{\sigma \to \infty} \tilde{P}(\sigma) = \overline{P}$$

Moreover, $\|M_f(s,\sigma)\|_{H_2}$ *tends to the infimum of* $\|M_f(s)\|_{H_2}$ *as* $\sigma \to \infty$, *i.e.*

$$\lim_{\sigma \to \infty} \|M_f(s,\sigma)\|_{H_2} = Trace\{F\overline{P}F'\}.$$

Proof : See [5]. ∎

In view of theorem 3, it is apparent that as σ takes on larger and larger values, the design algorithm given above generates a sequence of observer gains having the property that in the limit $\|M_f(s,\sigma)\|_{H_2}$ approaches the infimum of $\|M_f(s)\|_{H_2}$ over the set of all possible gains. A suboptimal solution would result with any chosen value of the parameter σ. However, for some particular class of systems, e.g. the well-known *regular problems* (i.e. D_{21} is surjective implying that Σ_{yw} is right-invertible and has no infinite zeros, and Σ_{yw} has no invariant zeros on the $j\omega$ axis), the infimum value of $\|M_f(s)\|_{H_2}$ can be achieved with the following observer gain [6],

$$K = B_{1,0} + \tilde{P}C'_{2,0}, \tag{39}$$

where $\tilde{P}$ is the positive semi-definite solution of

$$A_1\tilde{P} + \tilde{P}A'_1 - \tilde{P}C'_{2,0}C_{2,0}\tilde{P} + B_{1,1}B'_{1,1} = 0.$$

The resulting infimum value of $\|M_f(s)\|_{H_2}$ is given by,

$$\|M_f(s)\|_{H_2} = \text{Trace}\{F\tilde{P}F'\}.$$

Note that in this case, the observer gain K and thus the resulting recovery matrix is not parameterized as a function of σ. We note that for a regular problem when $\|M_f(s)\|_{H_2} = 0$, the observer gain K as given in (39) will achieve exact loop transfer recovery (ECLTR). However, to our knowledge, no optimization-based method exists in the literature to solve for the required gain that achieves $\|M_f(s)\|_{H_2} = 0$, whenever it is possible, for a general class of systems other than the class of regular systems. On the other hand, a direct design procedure

based on ATEA will yield an ECLTR design gain *whenever it can be done*; the algorithm is presented in subsection III.B.

Another special case of interest is as follows. Consider a left-invertible minimum-phase system Σ_{yw} which is non-strictly proper. Let the observer gain $K(\sigma)$ be given by

$$K(\sigma) = [B_{1,0},\ \sigma\tilde{P}(\sigma)C_{2,1}'],$$

where $\tilde{P}(\sigma) := \tilde{P}$ is the positive definite solution of

$$A_1\tilde{P} + \tilde{P}A_1' - \sigma\tilde{P}C_{2,1}'C_{2,1}\tilde{P} + B_{1,1}B_{1,1}' = 0.$$

It is simple to show that the observer gain $K(\sigma)$ given above achieves asymptotic closed-loop transfer recovery (ACLTR), i.e. the resulting $\|M_f(s,\sigma)\|_{H_2}$ tends to zero asymptotically as $\sigma \to \infty$. The above result has been given earlier by Chen *et al* [3].

It is of interest to investigate what type of time-scale structure and eigenstructure is assigned to the observer dynamic matrix A_o by the gain $K(\sigma)$ obtained via the algorithm given in equations (37) and (38). Clearly, the algorithm will make $M_-(s,\sigma)$, $M_b(s,\sigma)$ and $M_\infty(s,\sigma)$ zero as $\sigma \to \infty$, while shaping $M_e(s,\sigma)$ in a particular way so that the infimum of $\|M_f(s)\|_{H_2}$ is attained as $\sigma \to \infty$. In so doing, among all the possible choices for the time-scale structure and eigenstructure of A_o, it selects a particular choice which can easily be deduced from the results of cheap and singular control problems in [14] (see also, [17] and [9]). We have the following results.

1. As $\sigma \to \infty$, the asymptotic limits of the set of n_a^- eigenvalues $\Lambda_-(\sigma)$ and the associated set of left eigenvectors $V_-(\sigma)$ of A_o coincide respectively with the set of stable invariant zeros and the corresponding left state zero directions of Σ_{yw}. This renders $M_-(s,\sigma)$ zero as $\sigma \to \infty$.

2. As $\sigma \to \infty$, some of the n_b eigenvalues in $\Lambda_b(\sigma)$ coincide with the stable but uncontrollable eigenvalues of Σ_{yw} while the rest of them coincide with what are called 'compromise' zeros of Σ_{yw}

[14]. Also, the asymptotic limits of the associated left eigenvectors, namely $V_b(\sigma)$, fall in the null space of matrix $[B_1 - K(\sigma)D_{21}]'$ so that $M_b(s,\sigma) \to 0$ as $\sigma \to \infty$.

3. As $\sigma \to \infty$, the set of n_f eigenvalues $\Lambda_\infty(\sigma)$ of A_o tend to asymptotically infinite locations in such a way that $M_\infty(s,\sigma) \to 0$. The time-scale structure assigned to these eigenvalues depends on the infinite zero structure of Σ_{yw} (see for details in [14]). Also, the eigenvalues assigned to each fast time-scale follow asymptotically a Butterworth pattern.

4. As $\sigma \to \infty$, the asymptotic limits of n_a^+ eigenvalues in $\Lambda_e(\sigma)$ coincide with the mirror images of unstable invariant zeros of Σ_{yw}, while the associated set of left-eigenvectors of A_o coincide with the corresponding right input-zero directions of Σ_{yw}. The rest of n_c eigenvalues of $\Lambda_e(\sigma)$, as $\sigma \to \infty$, tend to some other finite locations, while the associated left-eigenvectors follow some particular directions. In the limiting process, it shapes the recovery matrix $\overline{M}_e(s)$ in a particular way so that the infimum of $\|M_f(s)\|_{H_2}$ is attained as $\sigma \to \infty$.

To conclude, we note that, as in the ATEA design procedure, the algorithm of equations (37) and (38) will render $M_-(s,\sigma)$, $M_b(s,\sigma)$ and $M_\infty(s,\sigma)$ zero asymptotically as $\sigma \to \infty$. Moreover, it shapes $M_e(s)$ in a particular way so that the infimum of $\|M_f(s)\|_{H_2}$ is attained as $\sigma \to \infty$. In contrast to this, ATEA design procedure of section III allows complete available freedom to shape the limit of recovery matrix $\overline{M}_e(s)$ in a variety of ways within the design constraints imposed by structural properties of the given system.

B. CLTR Design Via H_∞-Optimization

In this subsection, we consider H_∞-norm minimization of $M_f(s)$ or equivalently $T_{zw}^{au}(s)$. Unlike the case of H_2 -norm minimization in previous subsection, there are in general no direct methods available of exactly computing the infimum of $\|M_f(s)\|_{H_\infty}$, denoted here by γ^*. However, there are iterative algorithms that can approximate γ^*, at

least in principle, to an arbitrary degree of accuracy (See for example [8]). Recently, for a particular class of problems, i.e. when Σ_{yw} is left-invertible and has no invariant zeros on the $j\omega$ axis, such an infimum γ^* can be explicitly calculated [2].

We now proceed to present an algorithm for computing the observer-gain matrix K such that the resulting H_∞-norm of the recovery matrix $M_f(s,\gamma)$ is less than an a-priori given scalar $\gamma > \gamma^*$. The algorithm is as follows:

Step 0 : Choose a value $\epsilon = 1$.

Step 1 : Solve the following algebraic Riccati equation (H_∞-ARE),

$$A_1\tilde{P}+\tilde{P}A_1'-\tilde{P}C_{2,0}'C_{2,0}\tilde{P}-\frac{1}{\epsilon}\tilde{P}C_{2,1}'C_{2,1}\tilde{P}+B_{1,1}B_{1,1}'+\frac{1}{\gamma^2}\tilde{P}F'F\tilde{P}+\epsilon I_n = 0, \tag{40}$$

for $\tilde{P}$. Evidently, since (40) is parameterized in terms of γ, the solution $\tilde{P}$ will be a function of γ and is denoted by $\tilde{P}(\gamma)$.

Step 2 : If $\tilde{P}(\gamma) > 0$, then we proceed to **Step 3**. Otherwise, we decrease ϵ and go back to **Step 1**. Note that for $\gamma > \gamma^*$, it is shown in [18] that there always exists a sufficiently small scalar $\epsilon^* > 0$ such that the H_∞-ARE (40) has a unique positive definite solution $\tilde{P}(\gamma)$ for each $\epsilon \in (0, \epsilon^*)$.

Step 3 : Let

$$K(\gamma) = [B_{1,0} + \tilde{P}(\gamma)C_{2,0}', \ \frac{1}{2\epsilon}\tilde{P}(\gamma)C_{2,1}']. \tag{41}$$

We have the following theorem.

Theorem 4. *Consider a full-order observer-based controller with a gain determined from (41). Let $M_f(s,\gamma)$ be the resulting recovery matrix. Then, $\|M_f(s,\gamma)\|_{H_\infty}$ is strictly less than γ and tends to γ^* as $\gamma \to \gamma^*$.*

Proof : It follows simply from the results of [18]. ∎

Remark 4. *We note that γ acts here as a tuning parameter. Since at the beginning we do not know γ^*, it could very well happen that*

a chosen value of γ may turn out to be less than γ^*. In that case, the H_∞-ARE (40) does not have any positive definite solution even for sufficiently small ϵ. Then, one has to increase the value of γ and try to solve the H_∞-ARE once again for $\tilde{P}(\gamma) > 0$. One has to repeat this procedure as many times as necessary.

For the special case of *regular problems* defined in subsection IV.A, there exists a method of finding the gain that does not require the additional parameter ϵ. It is given by [6],

$$K(\gamma) = B_{1,0} + \tilde{P}(\gamma)C_{2,0}', \tag{42}$$

where $\tilde{P}(\gamma) := \tilde{P}$ is the positive semi-definite solution of

$$A_1\tilde{P} + \tilde{P}A_1' - \tilde{P}C_{2,0}'C_{2,0}\tilde{P} + B_{1,1}B_{1,1}' + \frac{1}{\gamma^2}\tilde{P}F'F\tilde{P} = 0,$$

such that $\lambda(A_1' - C_{2,0}'C_{2,0}\tilde{P} + \gamma^{-2}F'F\tilde{P}) \subseteq \mathcal{C}^-$. A full-order observer-based controller with gain obtained from (42) will produce a CLTR design such that $\|M_f(s,\gamma)\|_{H_\infty}$ is strictly less than γ.

Apparently, the gain $K(\gamma)$ obtained via the H_∞-optimization algorithm of equations (40) and (41) assigns a particular time-scale structure and eigenstructure to the observer dynamic matrix A_o. An investigation into the exact nature of time-scale structure and the eigenstructure of A_o as $\gamma \to \gamma^*$ is still an open research problem. But we like to point out that, as in the ATEA design procedure, the H_∞-optimization algorithm makes the corresponding $M_-(s,\gamma)$, $M_b(s,\gamma)$ and $M_\infty(s,\gamma)$ zero asymptotically as $\gamma \to \gamma^*$. Also, the corresponding $\overline{M}_e(s)$ is shaped in a particular way so that the infimum of $\|M_f(s)\|_{H_\infty}$ is attained as $\gamma \to \gamma^*$. In so doing, in addition to $\Lambda_\infty(\gamma)$, some elements of $\Lambda_e(\gamma)$ may be pushed to infinite locations in $\mathcal{C}^-$ as $\gamma \to \gamma^*$. Investigation of these and other properties of H_∞-optimization algorithm of equations (40) and (41) is outside the scope of this paper.

V. COMPARISON OF 'ATEA' AND 'ARE'-BASED DESIGN ALGORITHMS

A comparison is needed between optimal or suboptimal design schemes based on solving algebraic Riccati equations (ARE's) as described in

section IV and the asymptotic time-scale and eigenstructure assignment (ATEA) design schemes of section III. In this regard, our earlier paper [9] discusses several relative advantages and disadvantages of ATEA and ARE-based designs. Here, we examine ATEA design and optimization-based designs from two different perspectives: (i) numerical simplicity and, (ii) flexibility to use all the available design freedom.

Let us first consider the numerical aspects of both design methods. It is clear that the major part of optimization-based design algorithms of section IV lies in solving positive definite solution of a parameter-dependent ARE repeatedly for different values of the parameter σ or ϵ. It is well-known that these ARE's become numerically 'stiff' when the parameter takes on values that are close to a critical value. To be specific, the H_2-ARE becomes stiff as the parameter σ takes on larger and larger values, while the H_∞-ARE becomes stiff when γ approaches γ^*. This is due to the interaction of fast and slow dynamics inherent in such equations. Thus, the numerical difficulties occur not only due to the repetitive solution of ARE's but also due to the 'stiffness' of such equations. On the other hand, as evident from section III, ATEA adopts a decentralized design approach and in so doing alleviates both the problem of stiffness and the need for repetitive solution of algebraic equations. That is, in ATEA, interaction between the slow and various fast time-scales is isolated by working with the asymptotically finite and infinite eigenstructures in the observer dynamic matrix separately. The tuning parameter σ merely adjusts the relative size of different fast time scales and is introduced only parametrically in the construction of the final gain. Hence, this procedure presents no numerical difficulties whatsoever as the parameter takes on larger and larger values.

Another factor of importance in selecting a design procedure is its flexibility in addressing all the available design freedom. As summarized in section II, there exists considerable amount of freedom to shape the recovery matrix through eigenstructure assignment to the observer dynamic matrix A_o. Such a freedom can be utilized to shape $\overline{M}_e(s)$, the limit of the recovery matrix. Any optimization-based method adopts a particular way of shaping $\overline{M}_e(s)$ as dictated by the mathematical

minimization procedure. For example, as discussed earlier, in H_2 optimization $\overline{M}_e(s)$ is shaped by assigning some of the eigenvalues of A_o to the mirror images of the unstable invariant zeros of Σ_{yw}, while the associated set of left-eigenvectors of A_o coincide with the corresponding right input-zero directions of Σ_{yw}. Such a shaping obviously limits the available design freedom, and may or may not be desirable from an engineering point of view. Next, available design freedom can also be utilized to characterize appropriately the behavior of asymptotically infinite or otherwise called fast eigenvalues of A_o. What we mean by the behavior of fast eigenvalues is: (a) their asymptotic directions and, (b) the rate at which they go to infinity, i.e. the fast time-scale structure of A_o. As demonstrated in [9], the behavior of fast eigenvalues has a dramatic effect on the resulting controller bandwidth. Again, optimization-based design methods fix the behavior of fast eigenvalues in a particular way that may or may not be favorable to the designer's goals. We believe that the ability to utilize all the available design freedom is a valuable asset; in particular, exploring such a freedom in the case where complete recovery is not feasible is of dire importance. ATEA design methods of section III put all the available design freedom in the hands of designer and hence are preferable to optimization-based designs of section IV. However, a clear advantage of the optimization-based schemes is that at the onset of design, they do not require much systematic planning and hence are straightforward to apply. In fact, one simply solves the concerned ARE's repeatedly for several values of the tuning parameter until an appropriate suboptimal design is found. Admittedly, ATEA design does not have such a simplicity. One needs in ATEA design to come up with a careful utilization of the available design freedom and thus the selection of available design parameters that meet the practical design specifications. This can be done by a simple iterative adjustment. At each iteration, the required calculation in ATEA design procedure is straightforward and computationally inexpensive with added advantage that the algorithm does not involve solving any 'stiff' equations.

VI. NUMERICAL EXAMPLES

Control of flexible mechanical systems has been of interests in recent years. Presented in this section is a design example for closed-loop transfer recovery taken from the benchmark problem for robust control of a flexible mechanical system [16]. Although simple in nature, this problem will however provide us a design case where the concept of closed-loop transfer recovery can be fully illustrated. The problem is to control the displacement of the second mass by applying a force to the first mass as shown in figure 1 below. At the start, it is simple to verify that the basic open-loop system has a pair of degenerate eigenvalues at the origin and one pair of flexible modes. Equations for the dynamic

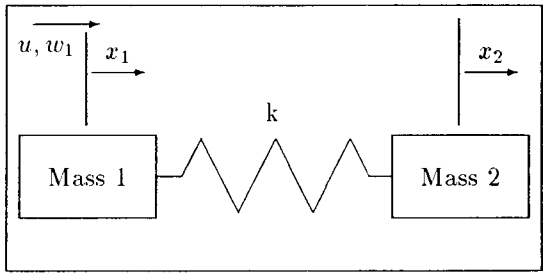

Figure 1: A Two-Mass-Spring Mass System

model are given below,

$$\begin{aligned} m_1\ddot{x}_1 &= k(x_2 - x_1) + u + w_1 \\ m_2\ddot{x}_2 &= k(x_1 - x_2) \end{aligned} \tag{43}$$

or

$$\begin{bmatrix} \dot{x}_1 \\ \dot{x}_2 \\ \dot{v}_1 \\ \dot{v}_2 \end{bmatrix} = \begin{bmatrix} 0 & 0 & 1 & 0 \\ 0 & 0 & 0 & 1 \\ -k/m_1 & k/m_1 & 0 & 0 \\ k/m_2 & -k/m_2 & 0 & 0 \end{bmatrix} \begin{bmatrix} x_1 \\ x_2 \\ v_1 \\ v_2 \end{bmatrix} + \begin{bmatrix} 0 \\ 0 \\ 1/m_1 \\ 0 \end{bmatrix} (u + w_1) \tag{44}$$

where $m_1 = m_2 = k_1 = k_2 = 1$, x_i, $i = 1, 2$, is the position of the i-th mass and v_i the velocity. The plant model used for robust control

synthesis and closed-loop transfer recovery is given by,

$$\dot{x} = \begin{bmatrix} 0 & 0 & 1 & 0 \\ 0 & 0 & 0 & 1 \\ -1 & 1 & 0 & 0 \\ 1 & -1 & 0 & 0 \end{bmatrix} x + \begin{bmatrix} 0 & 0 \\ 0 & 0 \\ 1 & 1 \\ 0 & -1 \end{bmatrix} \begin{bmatrix} w_1 \\ w_2 \end{bmatrix} + \begin{bmatrix} 0 \\ 0 \\ 1 \\ 0 \end{bmatrix} u \tag{45}$$

$$\begin{bmatrix} z_1 \\ z_2 \end{bmatrix} = \begin{bmatrix} 1 & -1 & 0 & 0 \\ 0 & 1 & 0 & 0 \end{bmatrix} x$$

The disturbance input w_2 and the controlled output z_1 are introduced as fictitious input and output variables to represent effects of the uncertain spring parameter k in a feedback setting [19]. The second controlled output z_2 is a performance variable whose response to a unit-impulse disturbance applied at w_1 must have a settling time of 15 seconds. To begin, we synthesize a state-feedback design for robust H_∞-control to variation in the spring constant k according to the results of [19] and define it as our target closed-loop transfer function . The full-state feedback gain matrix is given as follows,

$$F = [\,1.5059 \quad -0.4942 \quad 1.7379 \quad 0.93181\,] \tag{46}$$

Singular value plot of this closed-loop transfer function $T_{zw}(j\omega)$ is shown in figure 2. Transient responses to a unit impulse input $w_1 = \delta(t)$ are given in figure 3 showing that position response of the second mass has a settling time less than 15 *sec*, as specified in the design challenge problem of [16]. This state-feedback design is extremely robust to variation in the spring constant k; namely the closed-loop system remains stable for $0 < k < \infty$. Our design goal is to recover the performance achieved under this state-feedback design using output-feedback and full-order observer-based controllers in (5).

Before we enter into the synthesis of CLTR, it is important to note that the recovery is highly dependent on the structural properties between the selected set of measurement variables y and the disturbance inputs w. First of all, the analysis given in Part 1 [1] can be used to examine different possibilities in the measurement output selection for the closed-loop recovery. Table I summarizes the results of CLTR analysis for 7 sets of measurement variables. Note that the analysis points out

immediately that, with the target closed-loop transfer function being arbitrary, exact recovery (i.e ECLTR) is not possible. From the given set of sensors, only three of them (namely case c, case f and case g) can be used to achieve asymptotic recovery. That is, in these cases, one can design a full-order observer-based controller with high gain to recover the target closed-loop transfer function asymptotically. In subsection VI.A we present a CLTR design using the sensor set in case b. This set is the same as the one stated in [16] and the target closed-loop transfer function is unfortunately not recoverable in this case. Subsection 6.2 will present the results of an asymptotically recoverable design using the measurement set in case g. Notice that in the latter case, asymptotic recovery of the target transfer function $T_{zw}(s)$ can only be done with high observer gain.

A. Non-Recoverable Design Case

Let's consider the case where only measurement of position of second mass is available, i.e in case b of Table I where

$$C_2 = [0 \quad 1 \quad 0 \quad 0] \ , \ D_{21} = [0 \quad 0] \ , \ D_{22} = 0 \tag{47}$$

From Table I, we recognize immediately that there are severe limitations in the recovery design imposed by the presence of the $M_e(s)$-term with $n_c = 2$. Under this circumstance, there are clearly a variety of ways one can shape the term $\overline{M}_e(s)$ in our full-order observer-based controller designs. Thus, it is critical that one examines our design goals carefully in terms of defining the limit of recovery matrix $\overline{M}_e(s)$. It should be noted that of all the three methods presented, only the ATEA procedure can be used to arbitrarily shape the term $\overline{M}_e(s)$. Optimization-based methods will produce a limit of recovery matrix $\overline{M}_e(s)$ as discussed in section V. Table II shows a sequence of design possibilities using the three methods discussed in sections III and IV. Of course, within each design method, the generated sequence is parameterized by its own scalar tuning parameter; for example, in the ATEA design we invoke the tuning parameter σ with a properly selected time-scale structure, while in H_2- and H_∞-optimization meth-

ods the parameters are σ and γ respectively. Tendency of all these sequences of designs is to make the corresponding partitions $M_{-}(s,c)$, $M_b(s,c)$ and $M_\infty(s,c)$ zero as the tuning parameter c (i.e. $c=\sigma$ for the ATEA design and for H_2-optimization design, and $c=\gamma$ for the H_∞-optimization design) tends to the appropriate limiting value. As seen in figure 4, the norm of the observer-gain matrix $K(c)$ in these sequences of recovery designs grows unbounded even in the case where closed-loop transfer recovery is not possible. Shown below are the corresponding limiting recovery matrix $\overline{M}_e(s)$ for each of the design methods. In this example, the limit of recovery matrix for H_2-optimization is

$$\overline{M}_e(s)=\frac{[0.1499s+0.0376,\quad 0.0434s+0.0684]}{s^2+0.7071s+0.25} \tag{48}$$

while the one for the ATEA design is as follows,

$$\overline{M}_e(s)=\frac{[0.1082s+0.0122,\quad 0.0434s+0.0648]}{s^2+0.625s+0.08125} \tag{49}$$

For the H_∞-optimization, the corresponding limit of recovery matrix cannot be determined since one of the eigenvalues tends to infinity. Plots of the singular values of the recovery matrix $M_f(s)$ are shown in figure 5 for the limiting case (i.e corresponding to design case number 11 of Table II) in all three design methods. Notice that the curves corresponding to the ATEA and H_2 design cases approach the limit of recovery matrix $\overline{M}_e(s)$ given in equations (48) and (49) respectively.

Due to these differences in $\overline{M}_e(s)$, we have therefore different closed-loop transfer recovery error $E(s)$. The L_∞-norm of $E(s)$ is shown in figure 6 corresponding to every design case listed in Table II. Note that none of the design methods will yield ECLTR or ACLTR as evident from the analysis summarized in Table I. It clearly shows that the error cannot be made zero regardless of what method we use for the recovery design. However, depending on the way we select $\overline{M}_e(s)$, different design considerations can be traded-off in this non-recoverable case. For example, one design consideration is the robustness to variation in the spring constant k; the results are shown in figures 7 to 9 for the ATEA, H_2 and H_∞-optimization methods respectively. Clearly, due to its complete flexibility in selecting $\overline{M}_e(s)$, the ATEA design

procedure can be used to yield significantly better stability robustness. Transient responses to a unit impulse input in w_2 are shown in figures 10 to 12. Clearly, response peaks from all the output-feedback full-order observer-based controller designs are much higher than those achieved under state feedback. Results using optimization-based methods have the desired settling time of 15 sec. However, robustness of these designs are not as good as those from the ATEA design method which however exhibits a longer settling time. The example illustrates that there are many degrees of freedom in selecting $\overline{M}_e(s)$; the one shown here from the ATEA design is not meant to be the best among all possible choice of $\overline{M}_e(s)$. For example, one would need to modify $\overline{M}_e(s)$ if the settling time of 15 seconds is judged more important than the robustness consideration. An advantage of the ATEA method is that the observer design gain can be written explicitly in terms of the tuning parameter σ as follows,

$$K(\sigma) = \begin{bmatrix} 2.6562\sigma^2 - 4\sigma \\ 4\sigma \\ -3.9047\sigma^2 + 1.6 \\ 4.25\sigma^2 - 1.6 \end{bmatrix} \tag{50}$$

B. Asymptotically Recoverable Design Case

In this subsection, we consider the case where both position and acceleration of the second mass are available for feedback. The measurement output equation is given by

$$C_2 = \begin{bmatrix} 0 & 1 & 0 & 0 \\ 1 & -1 & 0 & 0 \end{bmatrix}, \; D_{21} = \begin{bmatrix} 0 & 0 \\ 0 & 0 \end{bmatrix}, \; D_{22} = \begin{bmatrix} 0 \\ 0 \end{bmatrix} \tag{51}$$

This corresponds to case g in Table I. Since $n_a^+ = n_c = 0$, the target closed-loop transfer function will be recoverable, but having $n_f = 4$ such a system can only recovered asymptotically. Furthermore, this implies that in all design methods the limit of recovery matrix $\overline{M}_e$ will be identically zero, and hence the H_∞-norm of the actual recovery error $E(s)$ approaches zero asymptotically as shown in figure 13. Table III shows a sequence of design possibilities from the three methods discussed in sections III and IV. Again the observer-gain in these sequences of designs for asymptotic recovery will become unbounded;

these results are shown in figure 14. Robustness results are shown in figures 15 to 17. Possibly, the significance of the ATEA design method lies in its flexibility to shape the design outcomes; for example, figure 15 shows that the ATEA design has significantly better robustness at the low-gain region where they can tolerate infinitely large change in the spring constant k. Transient responses to a unit-impulse input in w_1 are shown in figures 18 to 20. By increasing the observer gain, all the responses will approach those achieved under state feedback; this is to be expected for an asymptotically recoverable case (ACLTR). Again, in the ATEA method the observer design gain can be written explicitly in terms of the tuning parameter σ as follows,

$$K(\sigma) = \begin{bmatrix} 2\sigma & 2\sigma \\ 2\sigma & 0 \\ \sigma^2 & \sigma^2 - 1 \\ \sigma^2 & 1 \end{bmatrix} \tag{52}$$

VII. CONCLUSIONS

Presented in this paper are three design methods for closed-loop transfer recovery. Also discussed is the significance of each design method in terms of design simplicity, numerical difficulty and flexibility in utilizing the available design freedom to shape the limit of recovery matrix. All three methods of design provide explicit means of determining the appropriate observer gain matrix for closed-loop transfer recovery whenever it is possible. The design solution is usually characterized by a tuning parameter. In optimization-based methods, the gain is implicitly parameterized in terms of the solution of parameterized nonlinear algebraic Riccati equations (ARE's). On the other hand, ATEA design does not require solution of nonlinear algebraic equations. Here the tuning parameter enters the design solution only in the final step where we construct the composite observer gains from several subsystem designs. As the tuning parameter tends to its limiting value, a sequence of observer-based controllers is generated that yields in the limit a certain recovery matrix. For optimization-based methods, the limiting norm of the recovery matrix is simply the respective infimum

under H_2 (or H_∞)-optimization over all possible stabilizing observer gains. Optimization-based methods usually shape the recovery matrix in a particular way which may or may not be meaningful in an engineering point of view. Our experiences indicate that these designs have unnecessarily high gain than those achieved under the ATEA methods for a comparable size of the recovery error. Fundamentally, the ATEA method offers complete flexibility in shaping the recovery error utilizing all the available design freedom within the constraints imposed by the structural properties of the given system. In the case of exact closed-loop transfer recovery (ECLTR), the ATEA method can in all circumstances be used to obtain the appropriate observer design. By contrast optimization-based design approaches are simpler to use; however they are prone to numerical problems associated with solving "stiff" algebraic equations when the tuning parameters approach a certain critical limit. Different aspects of the CLTR design are illustrated in a numerical example for both a non-recoverable and a recoverable situations. All the design methods discussed in the paper have been implemented in a "Matlab" software package.

Acknowledgement

The work of B. M. Chen and A. Saberi is supported in part by Boeing Commercial Airplane Group and in part by NASA Langley Research Center under grant contract NAG-1-1210. The work of U. Ly is supported in part by NASA Langley Research Center under grant contract NAG-1-1210.

References

[1] B. M. Chen, A. Saberi and U. Ly, "Closed-Loop Transfer Recovery with Observer-Based Controllers – Part 1: Analysis," To appear in *Control and Dynamic Systems: Advances in Theory and Applications*, Academic Press, Inc. (1991).

[2] B. M. Chen, A. Saberi and U. Ly, "Exact Computation of the Infimum in H_∞-Optimization Via State Feedback," *Proceedings*

of The Twenty-Eighth Annual Allerton Conference, Monticello, Illinois, pp. 745-754 (1990).

[3] B. M. Chen, A. Saberi, S. Bingulac, and P. Sannuti, "Loop Transfer Recovery for Non-Strictly Proper Plants," *Control-Theory and Advanced Technology*, Vol. 6, No. 4, pp. 573-594 (1990).

[4] B. M. Chen, A. Saberi and P. Sannuti, "Loop Transfer Recovery for General Nonminimum Phase Non-strictly Proper Systems, Part 1 — Analysis," submitted for publication (1991).

[5] B. M. Chen, A. Saberi and P. Sannuti, "Loop Transfer Recovery for General Nonminimum Phase Non-strictly Proper Systems, Part 2 — Design," submitted for publication (1991).

[6] J. Doyle, K. Glover, P. P. Khargonekar and B. A. Francis, "State Space Solutions to Standard H_2 and H_∞ Control Problems", *IEEE Transactions on Automatic Control*, Vol. 34, No. 8, pp. 831-847 (1989).

[7] B. C. Moore, "On the Flexibility Offered by State Feedback in Multivariable Systems Beyond Closed Loop Eigenvalue Assignment," *IEEE Transactions on Automatic Control*, AC-21, pp. 689-692 (1976).

[8] P. Pandey, C. Kenney, A. Laub and A. Packard, "Algorithms for Computing the Optimal H_∞-Norm," *Proceedings of the 29th CDC*, Honolulu, Hawaii, pp. 2628-2689 (1990).

[9] A. Saberi, B. M. Chen and P. Sannuti, " Theory of ALTR for Nonminimum Phase Systems, Recoverable Target Loops, Recovery in a Subspace—Part 2: Design," *International Journal of Control*, Vol. 53, No. 5, pp. 1117-1160 (1991).

[10] P. Sannuti and A. Saberi," A Special Coordinate Basis of Multivariable Linear Systems - Finite and Infinite Zero Structure, Squaring Down and Decoupling," *International Journal of Control*, Vol.45, No. 5, pp. 1655-1704 (1987).

[11] A. Saberi and P. Sannuti, "Squaring Down of Non-Strictly Proper Systems," *International Journal of Control*, Vol. 51, No. 3, pp. 621-629 (1990).

[12] A. Saberi and P. Sannuti, "Time-Scale Structure Assignment in Linear Multivariable Systems Using High-gain Feedback," *International Journal of Control*, Vol.49, No. 6, pp. 2191-2213 (1989).

[13] A. Saberi and P. Sannuti, "Observer Design for Loop Transfer Recovery and for Uncertain Dynamical Systems," *IEEE Transactions on Automatic Control*, Vol. 35, No. 8, pp. 878-897 (1990).

[14] A. Saberi and P. Sannuti, "Cheap and Singular Controls for Linear Quadratic Regulators," *IEEE Transactions on Automatic Control*, AC-32, pp.208-219 (1987).

[15] A. A. Stoorvogel, "The Singular Linear Quadratic Gaussian Control Problem," Preprint, (1990).

[16] B. Wie and D. Bernstein,"A Benchmark Problem for Robust Control Design," *Proceedings of the 1990 American Control Conference*, May 23-25 (1990).

[17] Z. Zhang and J. S. Freudenberg, "Loop Transfer Recovery for Nonminimum Phase Plants," *IEEE Transactions on Automatic Control*, Vol.35, No.5, pp. 547-553 (1990).

[18] K. Zhou and P. Khargonekar, "An Algebraic Riccati Equation Approach to H_∞-Optimization," *Systems & Control Letters*, Vol. 11, pp. 85-91 (1988).

[19] B. Wie, Q. Liu and K-W Byun, "Robust H_∞ Control Synthesis Method and its Application to a Benchmark Problem," presented at the *1990 American Control Conference*, San Diego, California, May 23-25, 1990.

Table I: Analysis of Closed-Loop Transfer Recovery

Case	Measurement	n_a^-	n_a^+	n_b	n_c	n_f	CLTR
a	x_1	0	0	0	2	2	Non-recoverable
b	x_2	0	0	0	2	2	Non-recoverable
c	x_1 , x_2	0	0	0	0	4	Asymptotic Recoverable
d	x_1 , v_1	0	0	1	2	1	Non-recoverable
e	x_2 , v_2	0	0	1	2	1	Non-recoverable
f	x_1 , a_1	2	0	0	0	2	Asymptotic Recoverable
g	x_2 , a_2	0	0	0	0	4	Asymptotic Recoverable

Table II: Values of the Tuning Design Parameters (case b)

Design No.	ATEA	H_2-Optimization	H_∞-Optimization
	σ	σ	γ
1	0.75	1	1
2	1	10	0.9
3	2	10^2	0.8
4	3	10^3	0.7
5	4	10^4	0.6
6	5	10^5	0.5
7	6	10^6	0.4
8	7	10^7	0.3
9	8	10^8	0.275
10	9	10^9	0.25
11	10	10^{10}	0.225

Table III: Values of the Tuning Design Parameters (case g)

Design No.	ATEA	H_2-Optimization	H_∞-Optimization
	σ	σ	γ
1	0.25	1	1
2	0.5	10	0.9
3	1	10^2	0.8
4	2	10^3	0.7
5	5	10^4	0.6
6	10	10^5	0.5
7	15	10^6	0.4
8	20	10^7	0.3
9	30	10^8	0.275
10	40	10^9	0.25
11	50	10^{10}	0.225

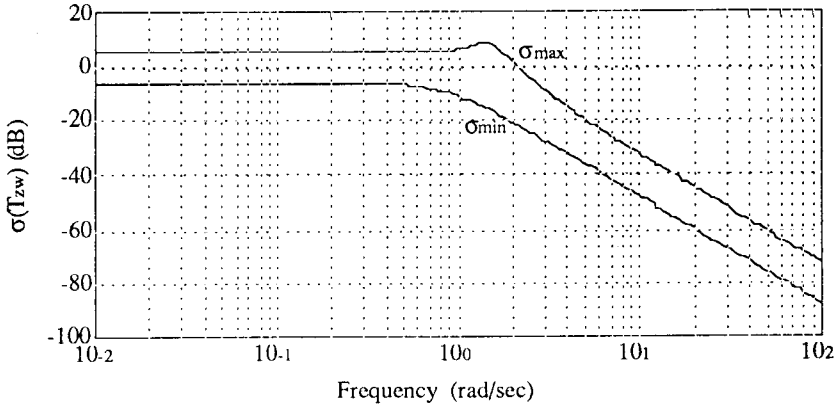

Figure 2: Singular Value Plot of Target Closed-Loop $T_{zw}(s)$

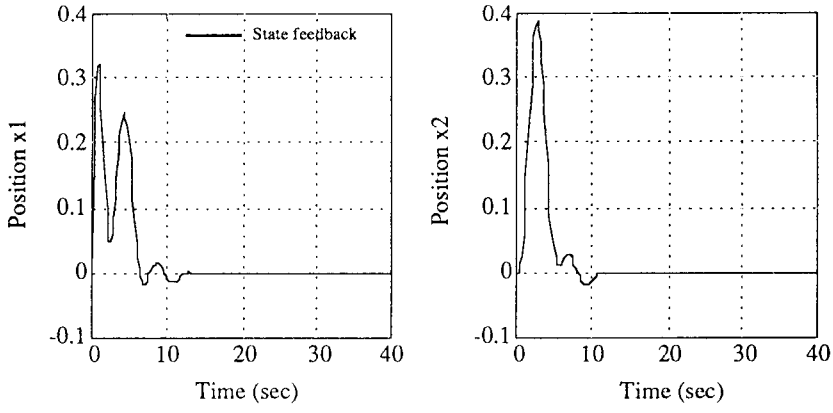

Figure 3: Impulse Responses in the Full-State Feedback Design

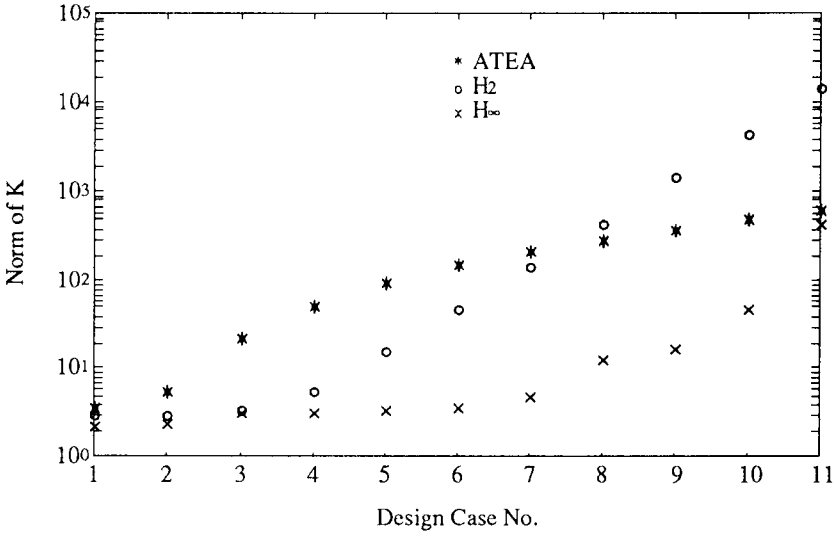

Figure 4: Norm of Observer Gain K for Designs in case b

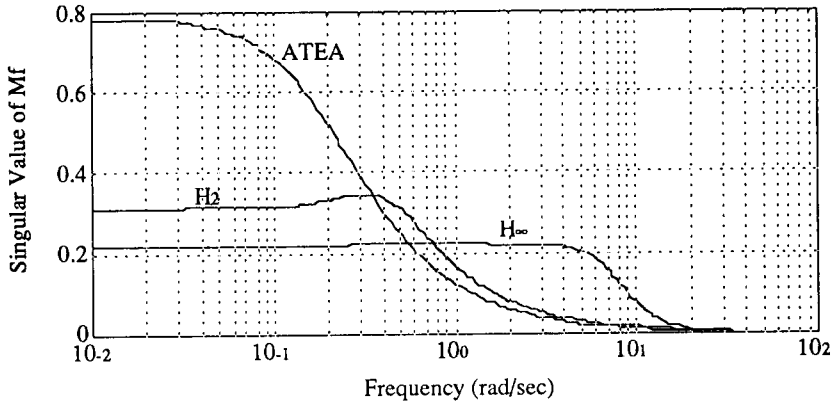

Figure 5: Singular Values of $M_f(s)$ for Design No. 11 (case b)

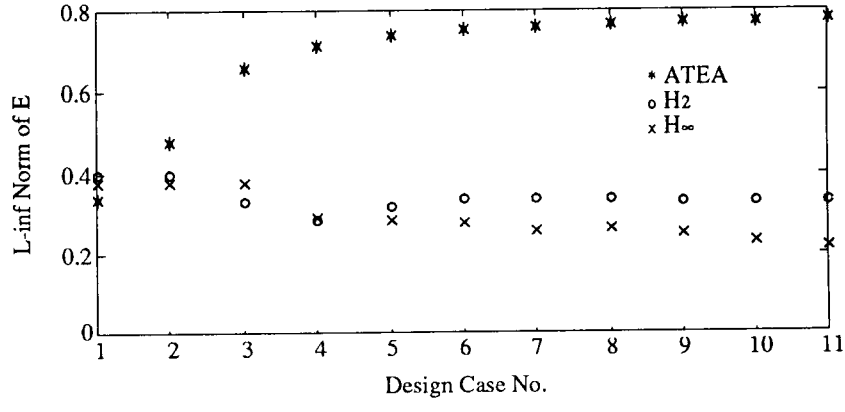

Figure 6: L_∞-Norm of $E(s)$ for Designs in case b

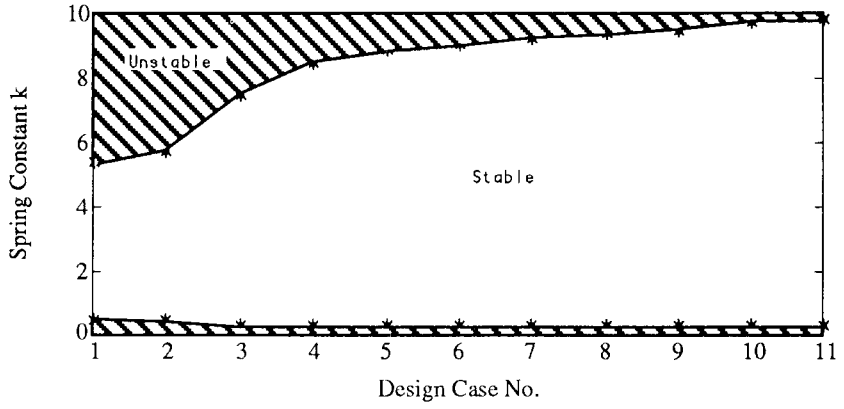

Figure 7: Robustness of ATEA Designs (case b) to Variation in k

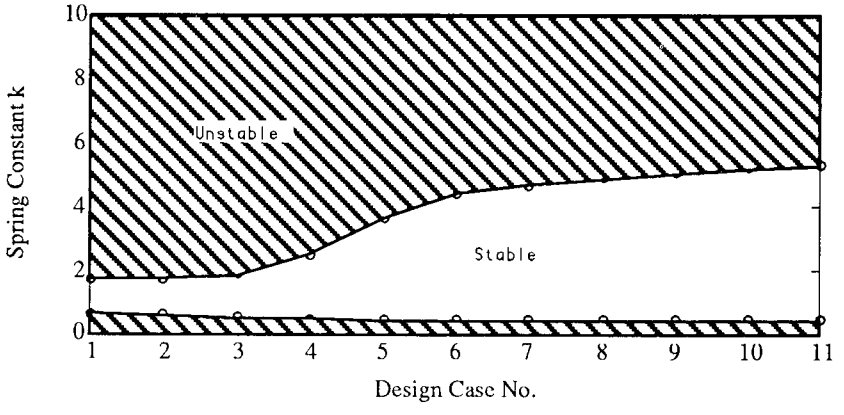

Figure 8: Robustness of H_2 Designs (case b) to Variation in k

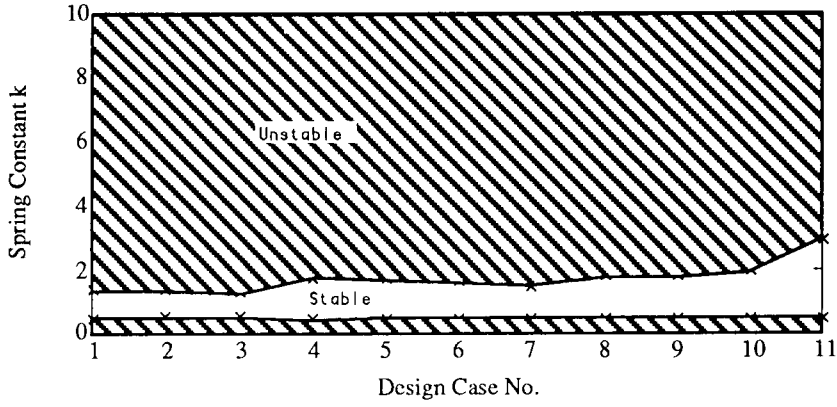

Figure 9: Robustness of H_∞ Designs (case b) to Variation in k

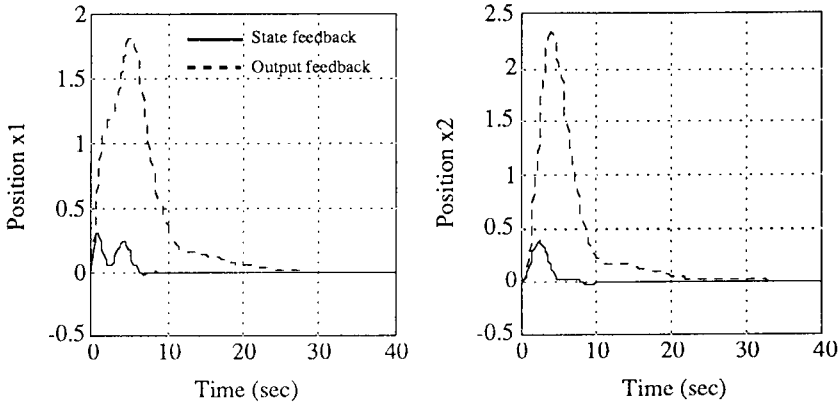

Figure 10: Impulse Responses for ATEA Design No. 1 (case b)

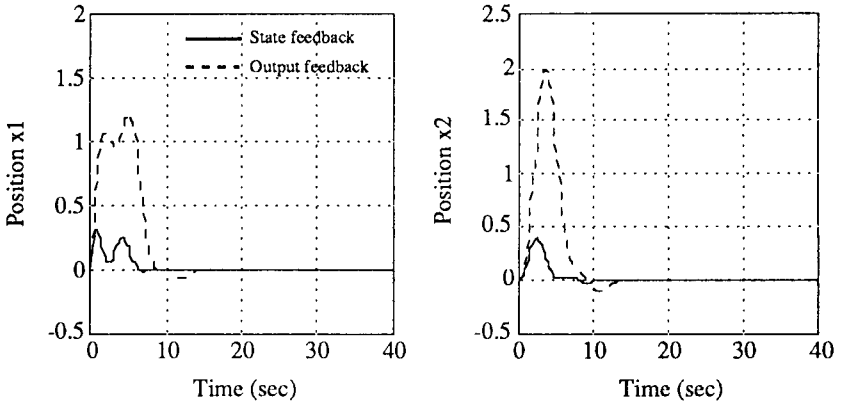

Figure 11: Impulse Responses for H_2 Design No. 3 (case b)

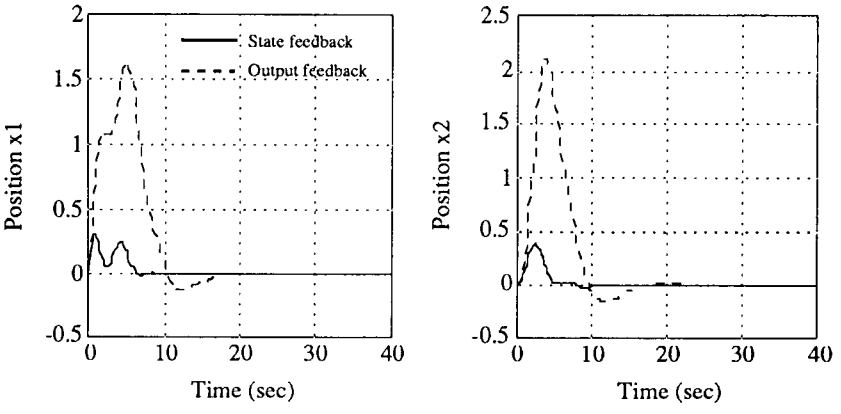

Figure 12: Impulse Responses for H_∞ Design No. 5 (case b)

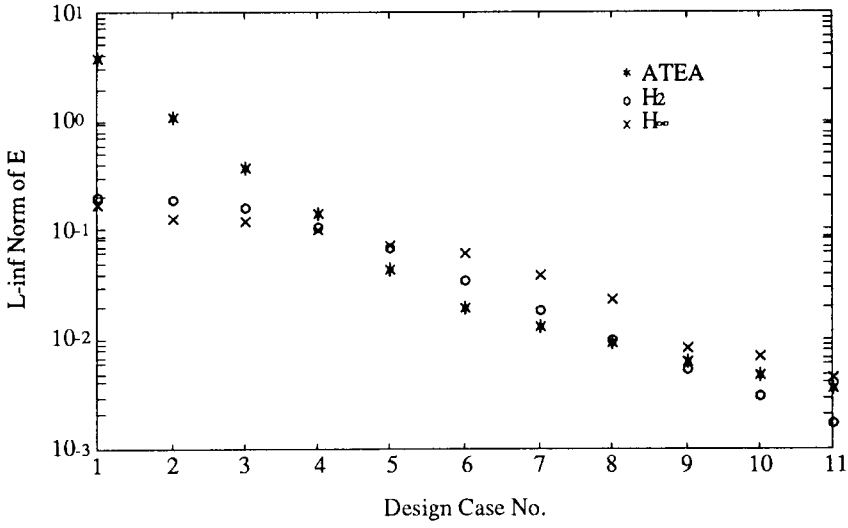

Figure 13: L_∞-Norm of $E(s)$ for Designs in case g

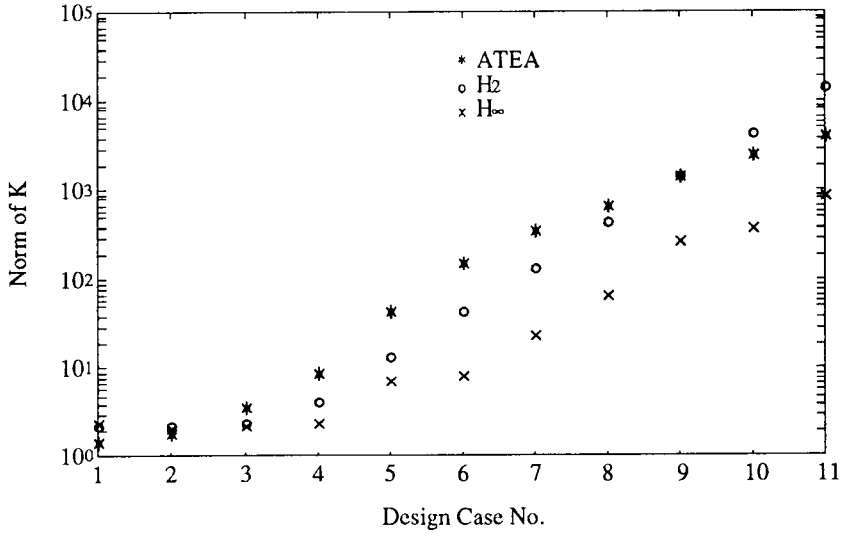

Figure 14: Norm of Observer Gain K for Designs in case g

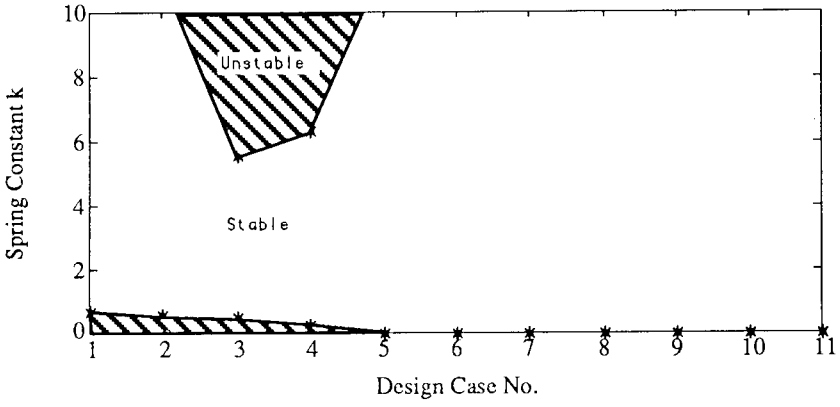

Figure 15: Robustness of ATEA Designs (case g) to Variation in k

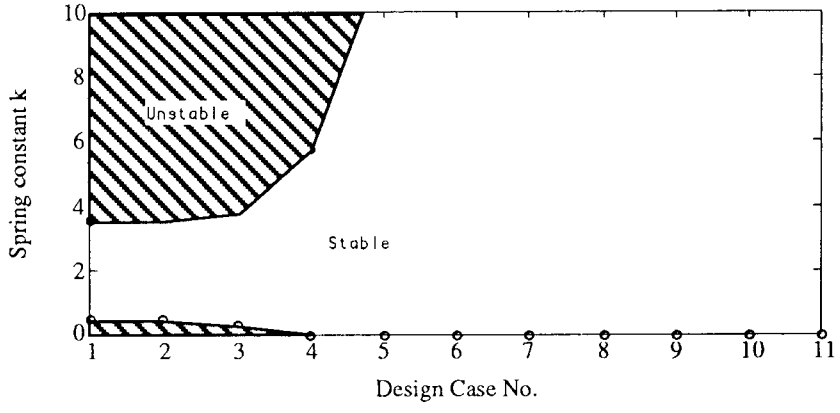

Figure 16: Robustness of H_2 Designs (case g) to Variation in k

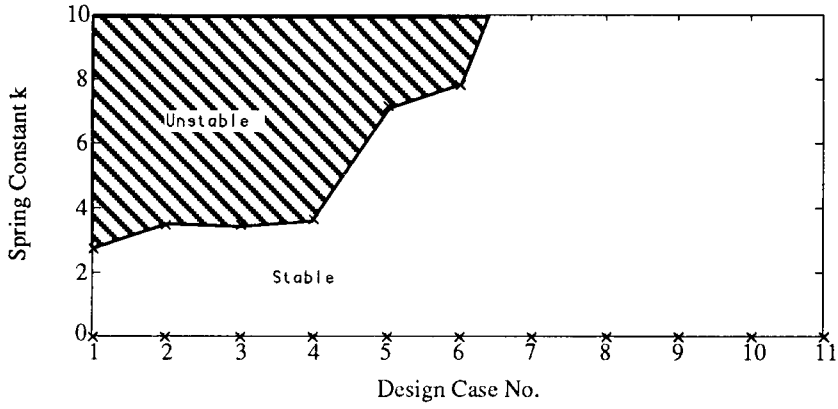

Figure 17: Robustness of H_∞ Designs (case g) to Variation in k

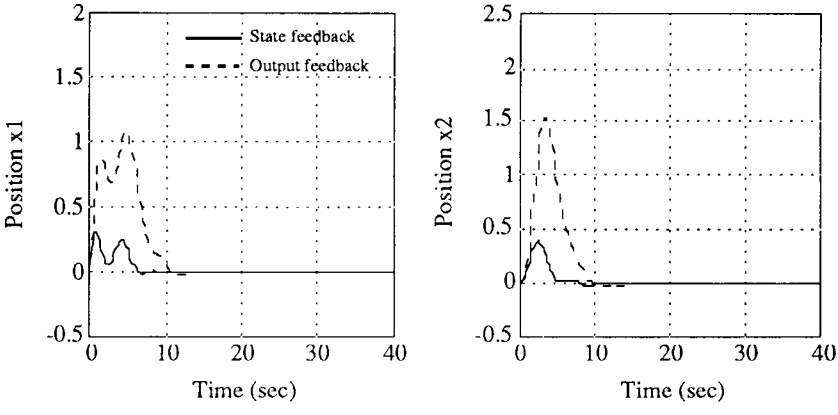

Figure 18: Impulse Responses for ATEA Design No. 3 (case g)

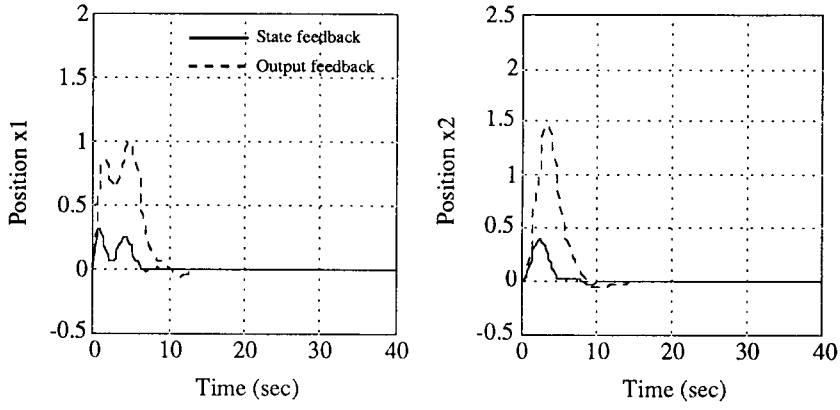

Figure 19: Impulse Responses for H_2 Design No. 3 (case g)

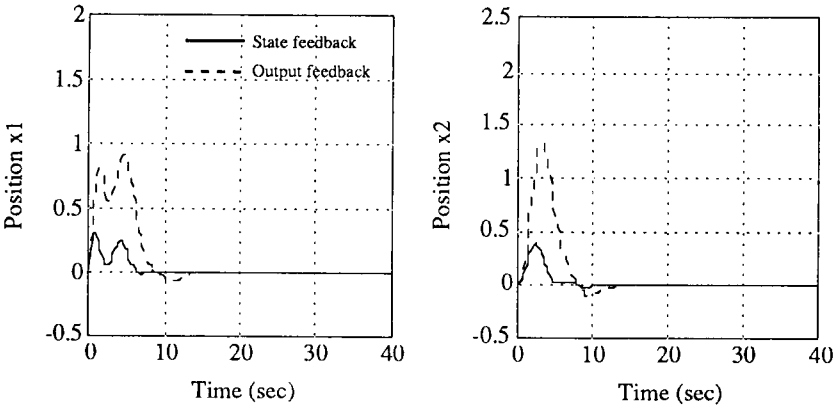

Figure 20: Impulse Responses for H_∞ Design No. 4 (case g)